NBSIR 80-2172

Estimating Safe Available Egress Time From Fires

Jacinto T. Collier

Center for Fire Research
National Engineering Laboratory
U.S. Department of Commerce
National Bureau of Standards
Washington, DC 20234

February 1981

Final Report

Prepared for
The Occupational Safety and Health Administration (OSHA)
Department of Labor
Washington, DC 20210

NBSIR 80-2172

ESTIMATING SAFE AVAILABLE EGRESS TIME FROM FIRES

Leonard Y. Cooper

Center for Fire Research
National Engineering Laboratory
U.S. Department of Commerce
National Bureau of Standards
Washington, DC 20234

February 1981

Final Report

Prepared for:
The Occupational Safety and Health Administration (OSHA)
Department of Labor
Washington, DC 20210

U.S. DEPARTMENT OF COMMERCE, Malcolm Baldrige, *Secretary*
NATIONAL BUREAU OF STANDARDS, Ernest Ambler, *Director*

PREFACE

This report on estimating safe available egress time from fires is one product of an ongoing joint research program of the Occupational Safety and Health Administration (OSHA) of the Department of Labor and the National Bureau of Standards (NBS), Center for Fire Research. The program is entitled: Key Elements of Emergency Escape Requirements for Employees in Workspaces Under OSHA Jurisdiction. Areas of research in this program include: Fire tests of stairwell-sprinkler systems; the relation of building design and human factors to emergency evacuation of workspaces; and studies of the smoke leakage of door assemblies.

TABLE OF CONTENTS

TABLE OF CONTENTS (Continued)

LIST OF TABLES

LIST OF FIGURES

NOMENCLATURE

A	area
c_1, c_2	constants defined below Eq. (4.8)
C_p	specific heat
f_h	a dimensionless heat transfer coefficient, see Eq. (A-1)
f_T	a dimensionless temperature, see Eq. (A-3)
g	acceleration of gravity
h	heat transfer coefficient
H	height of room
$\dot{m}_e$	rate of mass leaking from room
$\dot{m}_p$	rate of mass entrainment in plume
$\dot{q}$	a dimensionless value of $\dot{Q}$
$\dot{q}'_o$	$d\dot{q}/d\tau$ at $\tau = 0$
$\dot{Q}$	rate of fire's energy release
$\dot{Q}^*$	a dimensionless value of $\dot{Q}$
$\dot{Q}_{loss}$	amount of $\dot{Q}$ conducted out of room's bounding surfaces
$\dot{Q}_{other}$	a characteristic value of $\dot{Q}$
$\dot{Q}_{ceiling}$	convective heat transfer per Eq. (A-4)
r	radius
t	time
t_{EG}	$= t_{HAZ} - t_{DET}$
T	temperature
T_a	ambient temperature
$\bar{T}_p$	mixing cup temperature of plume crossection
$\bar{T}_h$	temperature corresponding to $\bar{\rho}_h$
T_{ad}	an adiabatic upper layer temperature

T_c	ceiling temperature
u	rate of heat transfer
Z	elevation
Z_i	elevation of interface
Δ	upper layer thickness
$\Delta\overline{T}_h$	$\overline{T}_h - T_\infty$
$\Delta\overline{T}_h^{(new)}$	a newly computed $\Delta\overline{T}_h$
ζ	dimensionless Z_i
ζ_o	ζ at $\tau = 0$
λ_c	$\dot{Q}_{loss}/\dot{Q}$
$\lambda_c^{(new)}$	a new estimate for λ_c
$\lambda_{ceiling}$	$\dot{Q}_{ceiling}/\dot{Q}$
λ_{other}	$\dot{Q}_{other}/\dot{Q}$
λ_r	effective fraction of $\dot{Q}$ radiated from combustion zone
ρ	density
ρ_a	ambient density
$\overline{\rho}_h$	average upper layer density
τ	dimensionless t
τ_{EG}	$\tau_{HAZ} - \tau_{DET}$
ϕ	$\overline{T}_h/T_\infty$
ϕ_o	ϕ at $\zeta = 0$
ξ	a dummy variable

Subscripts

DET	at detection
HAZ	at onset of hazardous conditions

ESTIMATING SAFE AVAILABLE EGRESS TIME FROM FIRES

Leonard Y. Cooper

Abstract

A general technique for estimating the time available for safe egress from a fire is presented. By introducing a qualitative and quantitative model of hazard development, the details of the technique are formulated for the room of fire origin problem. The inputs to the model are the area and ceiling height of the room, data from free burn tests of characteristic fuel assemblies likely to be found therein, the anticipated mode of fire detection, and a criterion for the onset of untenability. The output is an estimate of the length of time between detection of a fire and the onset of untenable conditions. Results of applying the estimation technique are presented and discussed.

Key words: Combustion products; compartment fires; egress; fire detection; fire growth; hazard analysis; mathematical models; room fires; smoke movement; tenability limits.

1. INTRODUCTION

1.1 Objective of the Study

The objective of this study is to develop a practical technique for estimating safe available egress times subsequent to the detection of a fire. Safe available egress time here means the interval between the

time of successful fire detection and alarm, and the time when hazardous conditions prevail in the given building space of interest.

Having obtained safe available egress time estimates for different spaces within a given building, a safe condition would be suggested if these estimates are of sufficient duration that people can escape the threatened space. The present study does not address the determination of whether or not such a safe condition exists. Rather, it provides the necessary input which, together with previous and ongoing research on human factors in egress, will allow such judgements to be made rationally.

To set the stage for the overall concept, assume that the following estimates have been established by a technically based calculation technique: For an ignition occuring in a given room located in a building equipped with a specific detector and alarm system, the available egress time from the room of fire origin is at least two minutes. Further, the available egress time in a corridor connected to the room of fire origin is at least four minutes. Finally, the available egress time in a third space, connected to the corridor is arbitrarily long (i.e., the third space is a place of refuge relative to a fire in the specific room of fire origin). Then based on the results of human factors studies, depending on the occupancy and dimensions of egress paths in the room of fire origin, and depending on the corridor and connecting doorway dimensions, it would be possible to determine whether a safe condition exists vis a vis a fire in the considered room of fire origin. A safe condition would exist if the time <u>required</u> for safe egress was equal to or less than the time <u>available</u> for safe egress. Determinations of this type when all spaces of the building are considered as potential rooms of fire origin would hopefully lead to an <u>overall</u> fire safe determination for the building.

It is the purpose of this study to develop a practical mechanism to establish the type of egress time estimates which were assumed in the above illustration.

It is appropriate to call attention to the work of Friedman [1][1] which, in a sense, serves as a prototype of the present investigation. By assuming exponential growth of fire in a fuel assembly, Friedman, in a simple but elegant manner, was able to tie together models for smoke or product of combustion generation and spread, for detection and alarm criteria, and for the development of untenable conditions. One result is a technique for estimating the ratio of safe available egress times, i.e., the relative hazard, of two different practical fuel assemblies. The present study adds more detail to the models of the various physical phenomena, thereby providing estimates for safe available egress times.

After briefly discussing overall concepts and methodology, this work specifically addresses the egress time problem for the room of fire origin. Future work will be devoted to detailing the adjacent (to room of fire origin) space and the overall building egress problem.

1.2 The Methodology

1.2.1 General Remarks

Procedures to estimate available egress time are developed from analytic models of fire development and smoke spread. The data base from full scale fire tests reported in the literature is also used. The analytic models are used to predict the significant features of growing and fully developed (flashed over) enclosure or compartment fires. In some practical way these models must take account of the characteristic fuel loads, the significant dimensions of the compartment and the various sorts of compartment openings which can affect fire ventilation; and which impact on spread of smoke.

Available tools for predicting compartment fire growth are in various stages of development. These tools can be divided into two groups, viz., those which are reliable, relatively simple and well

---

[1] Numbers in brackets refer to the list of references following this report.

supported by a strong data base, and those which are preliminary and are on the fringes of the state-of-the-art of fire technology. For example, while some quantitative predictions both of early growth stage and fully developed stage compartment fire phenomena can be made in many instances, simple but reasonably accurate predictions of transition state phenomena (e.g., flashover) are not yet possible.[2] Here, the transition state (flashover) refers to the linking state of fire development which starts when enclosure radiation feedback to the fuel significantly affects the burning rate of fuel, and which ends at the onset of fully developed fire conditions.

For the present purposes the details of transition stage phenomena are not required. There are two basic reasons why it is reasonable to assume that these details can be ignored. First, hazardous conditions for humans occur at room temperatures which are far lower than the levels that characterize the transition stage of fire development. In other words, for the purpose of studying life safety the problem of the room of fire origin is over (i.e., the room is intolerable for human occupancy) before the transition period is initiated.

Second, when available egress times from adjacent spaces are of interest; and where hazardous conditions in these spaces occur during or subsequent to the transition stage of fire development (in the room of fire origin) the time interval of the transition period is, in general, relatively short compared to the overall available egress time interval of interest. Accordingly, without loss of significant accuracy the problem of uncertain predictive capability for transition stage phenomena can be avoided by adopting a somewhat conservative model of real fire development. This model would predict a "lower limit" or "assured" available egress time. Such "lower limit" estimates would be obtained by assuming that fully developed stage fire conditions immediately follow

---

[2] Much progress has been made toward developing a capability for successful prediction of the details of transition stage phenomena. For example, see Emmons, et. al. [2].

early growth stage conditions (i.e., by conservatively shrinking the relatively brief transition stage phenomenology to a jump condition at a relatively early time in the fire scenario).

1.2.2 Rooms of Fire Origin

With a physical description of available ventilation paths in a given room of fire origin together with fuel load per unit floor area, reasonable models of fully developed fire energy release and its effect in adjacent spaces are available or can be constructed from results in the literature. However, for the early growth stages of fire development it is beyond the present stage of fire technology to calculate theoretically the history of energy release in practical fuel assemblies. Nevertheless, an existing data base from full scale free burn fire tests will be seen to yield useful quantitative energy release rate history estimates for a limited number of realistic fuel assemblies.

With a reasonable estimate of energy release rates during early stages of fire growth, it is possible to describe the time-dependent development of buoyancy driven plumes in fully or partially enclosed room-of-fire-origin spaces. Having first reached the ceiling, spreading across it and setting off fire detectors, the time interval required for the hot, smoky, toxic plume gases to drop to a hazardous elevation, one or one and a half meters (three or four feet) from the floor, or to reach a hazardous temperature can be estimated. Such time intervals will be taken as the safe available egress times for the room of fire origin.

1.2.3 Spaces Adjoining Rooms of Fire Origin

Having solved the available egress time problem in the room of fire origin, attention would be focused on solving the problem for adjacent spaces. The fire in the room of origin would still be assumed to be the source of hazardous combustion products. The rate at which these are driven into the adjacent space and the phenomenology of their dispersal

(e.g., stratification or uniform mixing) once they have entered this space must be predicted quantitatively. This would be possible once the ventilation paths of the room of fire origin have been established and appropriately described. These paths must include all significant penetrations in partitions between the room of fire origin and adjacent spaces.

The character of the ventilation paths impact on the adjacent space egress problem for two different reasons. First, the size of the fire in the room of origin will eventually be totally dependent on a ventilating oxygen supply from adjacent spaces (e.g., from a broken outside window). Second, the ventilation paths between the room of fire origin and the adjacent space under study result in smoke or product of combustion migration into the adjacent space and, ultimately, to the development therein of hazardous conditions. Even if these latter ventilation paths do not impact on the fire development, as in the case of securely closed doors (with, say, a broken window in the room of origin for fire ventilation), it is clear that they still affect the development of hazard in adjacent spaces. Indeed, as discussed by Cooper [3], leakage characteristics of door assemblies would play a key role in determining available egress times for the favorable (for adjacent space egress) circumstance of the "closed door" scenario.

The details of solution of the adjacent space problem are deferred to future work where the room of origin results developed here and all of the above ideas will be incorporated.

1.3 Order of the Remaining Sections

As noted above, the remainder of this report concentrates on a solution to the egress problem for the room of fire origin. Section 2 introduces the concept of characteristic fuel assemblies and explain the general utility of their free burn test data. Following this, a detailed description of the phenomenological model for hazard development is presented in section 3. Section 4 presents the quantitative aspects of

the overall qualitative phenomenology. The result of this presentation is an initial value problem, a (computer) solution of which yields the desired safe available egress time from a specified room of fire origin. Section 5 presents results obtained from using the latter, safe available egress time estimation technique. These results are discussed and compared to real fire scenarios. Finally, a summary of this investigation along with future directions is presented in Section 6.

2. FREE BURN TESTING OF CHARACTERISTIC FUEL ASSEMBLIES AND ITS UTILITY

2.1 Uncoupling of The Combustion Problem and the Flow Dynamics Problem

Heat and smoke sensitive fire detectors sound alarms and hazardous conditions develop in a building space as a result of products of combustion (POC) migrating from the combustion zone. As discussed in Section 1.2.1, for some significant time following ignition the development of the combustion process within this zone is essentially independent of the physical characteristics of the compartment which encloses the fire. This has an important implication in the solution to the problem at hand; namely, it is possible to uncouple the dynamics of the fire growth within the combustion zone from the flow dynamics occuring outside of this zone. This is the fire growth phenomenon that is the topic of this section.

2.2 The History of the Fire's Energy Release

For this analysis the most important characteristic of the fire is the history of its energy release. In particular, the portion of the energy which is convected away from the combustion zone provides the buoyancy force which ultimately drives the POC throughout the building space. In view of this, attention here is focused on the following question: When a fire is initiated in an assembly of combustible materials what is the history of the energy output as the fire develops

in a free burn situation? Free burn here is intended to suggest a burn of the fuel assembly in a large (compared to the combustion zone) ventilated space which contains a relatively quiescent atmosphere.

There are presumedly two possible ways to answer the above question; namely analytically or experimentally. As was indicated in Section 1, it is evident that for fire growth in practical fuel assemblies it is beyond the state-of-the-art of fire technology to expect the analytic approach to yield the required results. Thus, for the purpose at hand experimental methods must be used to answer the above question. A full scale free burn test of the fuel assembly is required.

2.3 The Practical Problem

If one seeks details of the growth of a fire in a specific fuel assembly, where the position and mechanism of the ignition is known, then no more need be added to the above approach. However, the objective of the present investigation is to provide broad based, practical insight on egress. The tools used to meet this objective would require the availability of data from fires developing from various possible ignitions in an arbitrarily large number of the myriad of fuel assemblies to be found in practice. However, for practical purposes the number of required full scale free burn tests must be limited. Accordingly it is appropriate to introduce the concept of limited numbers of fuel assemblies which are "characteristic" of occupancies of interest. Associated with each of these characteristic fuel assemblies would be a definite ignition scenario (maybe two scenarios) which are considered to be characteristic of the threat associated with the occupancy under consideration.

To illustrate, Figure 1 depicts a characteristic fuel assembly of the "type A" variety that one might associate with an office space occupancy (on the left), and an assembly of the "type A" variety that one might associate with a warehouse occupancy (on the right). With agreement on an appropriate ignition location and mechanism for each of these fuel assemblies, full scale free burns could be carried out in the

laboratory, and the desired energy release rate histories aquired. For the two fuel assemblies of Figure 1, one example of this later test process is depicted in Figure 2.

In practice, a data base for the energy release rate histories from a variety of characteristic fuel assembly free burn fires will have to be accumulated and catalogued. From a preliminary review of the literature of past full scale tests it is evident that the beginnings of this data base already exists. For example, Friedman [1] presents a table, reproduced here in Table 1, of exponential growth approximations to the energy release rate during free burn tests of a variety of practical fuel assemblies. Included in this table are the results of full scale fire tests of commodities stacked on pallets to a height of 4.6 m (15.1 ft) where the type of commodity was varied in each of seven separate tests. These results would prove useful in estimating safe available egress times from warehouse occupancies. Another accumulation of useful full scale test data on residential size fuel assemblies is provided by Pape et. al. [4]. There are, however, many "important" fuel assemblies whose energy release rates can not be reliably deduced from existing data in the literature. Full scale test programs for these will have to be formulated and carried out.

3. A QUALITATIVE DESCRIPTION OF THE PHENOMENA LEADING TO DETECTION AND HAZARDOUS CONDITIONS

3.1 General Remarks

As noted in section 2.1, for the times of interest, i.e., at least up to the time of untenable conditions in the room of fire origin, the combustion zone dynamics of a hazardous fire are basically uncoupled from POC migration. Also, from the ideas developed in sections 2.2 and 2.3 the energy release rate for a given fuel bed is known or obtainable. With this knowledge in hand, a quantitative dynamic model for POC migration and for fire detection and hazard development can be constructed. This section presents a qualitative description of this model.

3.2 Setting the Scene

For the purposes of the model, the geometry of the room of fire origin can be adequately described by its area and the height of its ceiling. The only restriction on the characteristic shape of the floor plan is that the space not have an unduly large length to width, or aspect ratio. Thus, for example, the model of POC migration to be adopted here may not be adequate for corridors with aspect ratios considerably larger than, say, 10:1. With regard to height of the room, it is consistent with the work of Baines and Turner [5] and with the upper, stably stratified, smoke layer model to be adopted here, that attention be restricted to spaces where the ratio of height to minimum horizontal dimension not exceed the order of one. Where either of these spatial restrictions are violated, it is possible that the phenomenological model to be adopted here will not be adequate.

It is assumed that all doors, windows and other significant partition penetrations to adjacent spaces are closed. It is also assumed that, prior to the onset of hazardous conditions, sufficient oxygen is available for free-burning combustion. These assumptions turn out to be conservative in the sense that under the conditions of a fully enclosed space and a free burning fire the model will generally estimate a more rapid development of hazardous conditions in the room of fire origin than would occur in practice if the room was unenclosed and/or if the effects of oxygen depletion on the fire were taken account of.

Even with all penetrations secured, there will be some leakage from the room of fire origin to adjacent spaces. This results from the expansion of the air heated by the fire's energy release. Even if sealed as tightly as practical, building enclosure partitions are generally unable to sustain significant overpressures without leaking. It is assumed that all this leakage occurs through leakage gaps which are close to the floor, i.e., the room leaks cool ambient air at a low elevation rather than high temperature products of combustion at a near-

ceiling elevation. Consistent with the work of Zukoski [6] and with the hazard development model to be adopted here, this latter assumption also turns out to be conservative vis-a-vis rapidity of the development of hazardous conditions.

Subject to the geometric restrictions and leakage assumptions, the potential room of fire origin under investigation is of arbitrary size. The space is assumed to be filled with fuel assemblies which are characteristic of the occupancy of interest. The potential fire threat is assumed to become a reality and the following scenario develops.

3.3 Ignition and Early Growth of the Fire

Time $t = 0$ is taken to be the time when an ignition is initiated in one of the fuel assemblies. The position and mechanism of the ignition is assumed to be similar to the ignition which initiated the free burn fuel assembly test referred to earlier. Indeed, for all $t \geq 0$, of interest here, the combustion zone dynamics of the ensuing enclosure fire are assumed to be substantially similar to the combustion zone dynamics in the related free burn test. In other words, the energy release rate history will remain close to that of the free burn test up to, and somewhat beyond the time of hazardous conditions.

For the two different fuel assembly types of Figure 1, the scenario at ignition is depicted in Figure 3. As suggested in that figures, the power level of many common ignition sources will likely be in the order of 10 kW. This corresponds to typical power levels of small wastepaper basket type fires.

Time moves on. Because of the temperature of the POC, buoyancy forces drive them out of the growing combustion zone and up toward the ceiling. In this way a plume of upward moving elevated temperature gases is formed above the fire. All along the axis of the plume relatively quiescent and cool gases are laterally entrained and mixed with

the plume gases as they continue their ascent to the ceiling. As a result of this entrainment the total mass flow in the plume continuously increases and the average temperature in the plume continuously decreases with increasing height. The plume dynamics at any instant of time can, with reasonable accuracy, be quantitatively described by a simple function of the rate of energy release from the combustion zone.

When the plume gases impinge on the ceiling they spread across it forming a relatively thin, stably stratified upper layer. As the plume gas upward filling process continues, the upper gas layer grows in depth and the relatively sharp interface between it and the cool ambient air layer below continuously drops. Thus, this interface separates a potentially hazardous mixture of POC and previously entrained air above, from cool ambient air below which, as yet, is assumed not to have been affected by the fire. It is possible to estimate the rate of drop of this interface as a function of its instantaneous vertical position and of the then current picture of the plume dynamics, i.e., the current rate of fire energy release. By making the reasonable engineering assumption that the upper layer is always fully mixed or homogeneous, it is also possible to estimate it's average temperature.

3.4 Detection

The fire and POC migration phenomena described in the last paragraph continue; and presumedly before hazardous conditions prevail in the space, the fire is detected. The criteria by which one might model the detection event would have to be based on the performance characteristics of the particular detector device being used, and on the characteristics of the changing POC environment which engulfs the device and which leads to its activation.

With regard to the POC environment, the present phenomenological model provides a dynamic description in terms of thickness and temperature of an assumed homogeneous upper layer. However, estimates for

these parameters during times when the layer is theoretically very thin cannot be considered as reliable. Indeed, the "uniform upper layer" concept is not even valid until such time during the course of the fire that such a layer would totally submerge the ceiling jet. And these ceiling jets can be of the order of ten percent of the ceiling height [7]. In short, until such times during the course of the fire when estimated upper layer thicknesses have reached the order of one foot (assuming ceiling heights of the order of ten feet) such estimates and their associated temperatures are unreliable for use in detection criteria.

Where detectors are spaced with reasonable density and in a regular grid (e.g., according to the specification of Benjamin, et al. [8]) across rooms with relatively smooth ceiling surfaces, detection criteria of the type developed by Alpert [9] from results of his analysis of ceiling jet flows [7] may be applicable. The experimental data of Heskestad and Delichatsios [10,11] and their correlations [12,13] would also be useful in this regard.

Analysis of detector response by using any of the latter references [8-13] would be based on knowledge of the environment within the ceiling jet and at the detector location. When the spacing of the detectors, i.e., the distance of a detector from the fire, is too great (depending on the fire growth rate, ceiling smoothness and the height of the room) these environments are not generally well known. Under such sparsely deployed detector scenarios, there are potentially useful and practical detection criteria that can be constructed from the geometric specifications of the room of fire origin and from knowledge of the instantaneous values of the fire energy release rate, layer thickness, and layer temperature. For example, it may be reasonable to expect that an upper smoke layer greater than some specified thickness would activate an appropriately sensitive smoke detector. Alternatively, if a heat sensitive detector were deployed its time of activation could be estimated with the use of the history of the layer temperature. It is important to point out that these latter types of detection are strictly speculative,

and, their reliability has not been evaluated in practice.

Detection without an actual detection and alarm device is also possible. This could result from human sensitivity to, say, visual obscuration due to smoke or downward directed thermal radiation both of which would develop with increased overhead layer growth and fire intensity. If appropriate levels of the effects can be identified, it would be a simple matter to use these criteria for estimating the time of fire detection.

Whatever detection criteria are finally used in practice, their validity should clearly be verified with appropriate measurements. Such verification would constitute a major future activity which will be required to support the validity of the concepts being introduced here.

The results of applying some of the above hypothetical detection criteria is discussed in a later section.

Figure 4 depicts a possible state of affairs within the overall fire growth scenario at the time of detection. The actual condition would be a function of the arrangement and type of detector. The detection event could occur at an earlier or later state of fire development. What is important to this model is that detection does in fact occur, thereby starting the "clock" which ultimately measures the available egress time.

3.5 Intermediate Times - Between Detection and Hazard

Having attained detection (and, presumedly, alarm) the "human factors" aspect of egress would be initiated. In the meantime the upper layer continues to grow in both depth and temperature. The energy release rate of the fire continues to be very close to that of the free burn test. Most important, safe evacuation is still possible. Figure 5 depicts the situation at some intermediate time between detection and hazard.

3.6 The Approach of Hazardous Conditions

The scenario continues to develop. Eventually the conditions in the space become hazardous beyond human tolerability. As with the situation for detection criteria, the criteria which define the onset of hazardous conditions must be quantitatively related to those physical parameters for which the model can provide reasonable estimates. Again, the upper layer thickness (or the vertical position of it's interface), and it's temperature can be used to provide the measures of whether or not the hazardous conditions prevail.

The implications of interface position on hazard are clear. Above the interface the gases are smoky, and, therefore, potentially obscure beyond reasonable visibility. They are contaminated with toxic POC and, therefore, they are themselves at toxicity levels potentially beyond human tenability. Below the interface the gases are modeled as cool, uncontaminated, ambient air. If the interface drops below some preassigned level, say some position between one to one and a half meters (three to four feet), it is not practical to expect people to be capable of keeping their faces out of the potentially hazardous upper layer. Thus, a simple, albeit conservative, criterion for hazard can be established which is independent of the details of the toxicity and smoke production properties of the constituent materials making up the fuel assembly. Namely, once the upper layer - lower layer interface drops to a preassigned level, hazardous conditions begin to prevail in the room of fire origin and safe evacuation is no longer likely. Further work will take account of the actual POC dilution and the resulting hazard level of the upper layer gases.

As it happens, a high temperature upper layer condition can, in and of itself, lead to hazardous conditions even before the interface drops to a hazardous level. This would occur by virtue of its emission of untenably high levels of thermal radiation. For example, Babrauskas [14] has reviewed the literature and found that the threshold of human

tenability to heat fluxes for extended periods of time falls in the range of 1.2 kW/m^2 to 2.5kW/m^2. The latter value corresponds to radiation from a black body at 183°C (361°F). Thus, this general temperature (radiation) level, which is well below temperature (radiation) levels generally associated with flashover phenomena, would appear to form the basis for a second independent criterion for hazard. Namely, once the upper gas layer temperature reaches some preassigned high value, hazardous conditions begin to prevail in the room of fire origin and safe evacuation is no longer likely.

Taking the above two criteria together, the following overall criterion for untenability results: The room of fire origin is assumed to be untenable for safe evacuation at such time that either (1) the upper layer interface drops to some specified, low hazardous level, or (2) the temperature of the upper level grows to some specified, high, hazardous value.

Figure 6 depicts the state of affairs in the room of fire origin at the time when untenable conditions begin to prevail. In the left hand office occupancy, the low level of the interface was the initiator of hazardous conditions. In the right hand warehouse occupancy, however, it was a hazardous level of radiation from the upper layer that triggered the onset of untenability.

4. QUANTITATIVE DESCRIPTION OF THE MODEL - THE GOVERNING EQUATIONS

4.1 General Remarks

The previous section presented a qualitative description of the events occuring in a building space subsequent to the initiation of a fire and up to the time that hazardous conditions prevail. This section constructs a quantitative description of this model. The major elements of this will include the turbulent buoyant plume theory of Morton et. al. [15] together with the experimental plume results of Yokoi [16], the

theory of Baines and Turner [5] on the dynamics of such plumes in confined spaces, and Zukoski's [6] application of this latter theory to the fire problem. Figure 7 presents a simple illustration of the flow dynamics described.

4.2 Formulation of the Initial Value Problem for Temperature of the Upper Layer and Position of the Interface

As noted earlier, the partitions of the room of fire origin are assumed to have all major penetrations (e.g., doors, windows, and vents) closed. Any leakage from the room resulting from fire driven gas expansion is assumed to occur near the floor level. The sketch of Figure 7 is compatible with these assumptions, both of which lead to some conservatism in the eventual prediction of the time for onset of untenability.

The fire's combustion zone is modeled as a point source of energy release which is effectively located at the floor level. The mass rate of fuel introduced from this zone into the plume is neglected compared to the mass flow rate of entrained air. Except for the buoyancy forces that they produce, density variations in the flow field are neglected (e.g., the Boussinesq approximation is invoked in the usual manner). Using the fact that the absolute pressure throughout the space varies only insignificantly from a constant uniform value [6], the density can be related to the temperature at any time and spatial position through the perfect gas law according to

$$\rho T = \text{Constant} = \rho_a T_a \tag{4.1}$$

where ρ_a and T_a are the density and absolute temperature, respectively, of the ambient air.

The total time varying energy release rate of the combustion zone is defined by $\dot{Q}(t)$. The fraction of $\dot{Q}$ which effectively acts to heat plume gases and to ultimately drive the plume's upward momentum is $(1-\lambda_r)$ where λ_r is approximately the fraction of $\dot{Q}$ lost by radiation from the

combustion zone and plume.

Following Zukoski [6], and Zukoski, Kubota, and Cetegen [17], the total mass flow in the plume, $\dot{m}_p$, and the mass mixing cup temperature of the plume, $\overline{T}_p$, at a distance Z above the fire (but below the layer interface) can be estimated by

$$\overline{T}_p/T_a - 1 = (\dot{Q}^*)^{2/3}/0.210$$

$$\dot{m}_p = 0.210\rho_a(gZ)^{1/2}Z^2(\dot{Q}^*)^{1/3} \qquad 0 < Z \leq Z_i(t) \qquad (4.2)$$

where $\dot{Q}^*$ is defined as

$$\dot{Q}^* = (1-\lambda_r)\dot{Q}/[\rho_a C_p T_a (gZ)^{1/2}Z^2]$$

and where g is the acceleration of gravity and C_p is the specific heat of the ambient air. The mass flow rate of ambient air, $\dot{m}_e$, leaking out of the room's lower leakage paths is given by [6]

$$\dot{m}_e = (1-\lambda_c)\dot{Q}/(C_p T_a) = [(1-\lambda_c)/(1-\lambda_r)]\dot{Q}^*\rho_a(gH)^{1/2}H^2 \qquad (4.3)$$

where λ_c is the instantaneous fraction of $\dot{Q}$ lost to the bounding surfaces of the room and it's contents (i.e., $\lambda_c = \dot{Q}_{loss}/\dot{Q}$) and where $\dot{Q}^*$ is evaluated at $Z = Z_i(t)$; $Z_i(t)$ being the time varying distance of the interface above the fire. This total energy loss characterized by λ_c occurs as a result of a variety of different convective and radiative heat transfer interchanges between the room's gases and the above mentioned surfaces.

A mass balance for the lower (shrinking) volume of ambient air results in

$$\frac{d(\rho_a A Z_i)}{dt} + \dot{m}_e + \dot{m}_p(Z = Z_i) = 0$$

where A is the area of the room of fire origin, and where estimates for $\dot{m}_e$ and $\dot{m}_p$ are provided in Eqs. (4.2) and (4.3).

An energy balance for the upper layer results in

$$\int_o^t (1-\lambda_c)\dot{Q}dt = \int_{Z_i}^H \rho A(C_p T - C_p T_a)dZ$$

where H is the height of the room. Using Eq. (4.1) in the above, and defining the average upper layer density, $\bar{\rho}_h$, as

$$\bar{\rho}_h = \frac{1}{(H-Z_i)} \int_{Z_i}^H \rho dZ \tag{4.5}$$

the following results

$$1 - \bar{\rho}_h/\rho_a = 1 - T_a/\bar{T}_h = [\int_o^t (1-\lambda_c)\dot{Q}dt]/[\rho_a C_p T_a A(H-Z_i)] \tag{4.6}$$

Here, $\bar{T}_h$ is defined as the temperature corresponding to $\bar{\rho}_h$ through Eq. (4.1). When the upper layer is well mixed, $\bar{\rho}_h$ and $\bar{T}_h$, computed in accord with the above, should provide a reasonable estimate for the hot layer's actual density and temperature. This uniformly mixed upper layer model will be assumed to provide an accurate representation of the actual phenomena under investigation.

For the present purpose it is convenient to introduce the following dimensionless forms for t, Z_i, $\bar{T}_h$, and $\dot{Q}$

$$\tau = t/t_c \quad ; \quad \zeta = Z_i/L_c$$

$$\phi = \bar{T}_h/T_a \quad ; \quad \dot{q} = \dot{Q}/\dot{Q}_o \tag{4.7}$$

where t_c and L_c are a characteristic time and length, respectively. Also, $\dot{Q}_o$ represents some characteristic energy release rate. For example, provided it is nonzero, $\dot{Q}_o$ will be taken as $\dot{Q}(t=0)$. These are now introduced into Eqs. (4.2) - (4.4) and (4.6), where Eq. (4.6) is recast

into differential form. After some manipulation the following pair of governing equations for the dimensionless interface position, ζ, and upper layer temperature, ϕ, results

$$\frac{d\zeta}{d\tau} = -c_1\dot{q} - c_2\dot{q}^{1/3}\,\zeta^{5/3}$$

$$\frac{d\phi}{d\tau} = \phi[c_1\dot{q} - (\phi-1)c_2\dot{q}^{1/3}\,\zeta^{5/3}]/(\zeta_o - \zeta) \tag{4.8}$$

where $\zeta_o = H/L_c = \zeta(\tau = 0)$

and where $c_1 = \dfrac{(1-\lambda_c)\dot{Q}_o t_c}{\rho_a C_p T_a A L_c}$

$$c_2 = \frac{0.210 t_c}{A}\left[\frac{(1-\lambda_r)\dot{Q}_o g L_c^2}{\rho_a C_p T_a}\right]^{1/3}$$

For ρ_a, T_a, C_p and g values of

$\rho_a = 0.0735$ lb/ft^3 = 1.18 kg/m^3

$T_a = 530°R = 294°K$

$C_p = 0.24$ BTU/(lb°F) = 240 cal/(kg°C)

$g = 32$ ft/sec^2 = 9.80 m/sec^2

the values of c_1 and c_2 are

$$c_1 = 0.107(1-\lambda_c)(\dot{Q}_o/\text{kW})(t_c/\text{sec})(\text{ft}/L_c)^3/(A/L_c^2)$$

$$c_2 = 0.314(t_c/\text{sec})[(1-\lambda_r)(\dot{Q}_o/\text{kW})(\text{ft}/L_c)^4]^{1/3}/(A/L_c^2)$$

The problem now becomes one of simultaneously solving the above pair of differential equations subject to the appropriate initial conditions. For the present purposes these initial conditions can be taken as those relating to one of two different cases.

Case 1: $\dot{q}(\tau=0) = 1$, i.e., $\dot{Q}(t=0) \neq 0$.

Here define

$$\dot{q} = \dot{Q}(t)/\dot{Q}(t=0) \tag{4.10}$$

and assume

$$\lim_{\tau\to 0} \dot{q} = 1 + \dot{q}_o' \tau + 0(\tau^2) \tag{4.11}$$

where $\dot{q}_o' = d\dot{q}/d\tau$ at $\tau = 0$

Then solve Eqs. (4.8) subject to

$$\zeta(\tau=0) = \zeta$$

$$\phi(\tau=0) = \phi_o = 1+\zeta_o^{-5/3} c_1/c_2 \tag{4.12}$$

where analysis of the apparent singularity of the second of Eqs. (4.8) leads to the result that the initial value of $d\phi/d\tau$ can be obtained from

$$\lim_{\tau\to 0} d\phi/d\tau = \{(c_1/c_2)[2\dot{q}_o'+5(c_1+c_2\zeta_o^{5/3})]/(6\zeta_o^{8/3})\}[1+0(\tau)] \tag{4.13}$$

Case 2: $\dot{q}(\tau=0) = 0$, i.e., $\dot{Q}(t=0)=0$

Here assume

$$\lim_{\tau\to 0} q = \dot{q}_o'\tau+0(\tau^2) \tag{4.14}$$

Then solve Eqs. (4.8) subject to the initial conditions

$$\zeta(\tau=0)=\zeta_o, \ \phi(\tau=0)=\phi_o=1 \tag{4.15}$$

Here analysis of the problem reveals the following small time estimates for ζ and ϕ

$$\lim_{\tau \to 0} \zeta = \zeta_o - (3/4) c_2 (\dot{q}_o)^{1/3} \zeta_o^{5/3} \tau^{4/3} [1 + O(\tau^{2/3})]$$

$$\lim_{\tau \to 0} \phi = 1 + (2/3)(c_1/c_2)(\dot{q}_o')^{2/3} \zeta_o^{5/3} \tau^{2/3} [1 + O(\tau^{2/3})] \qquad (4.16)$$

4.3 Safe Available Egress Time From the Solution to the Initial Value Problem

The above initial value problem for ϕ and ζ would be solved by a numerical integration procedure. Compatible with the hazard criterion of the type described in section 3.6, the actual solution procedure would be terminated in a given problem at that time,

$$t_{HAZ} \qquad \text{i.e.,} \qquad \tau_{HAZ} = t_{HAZ}/t_c \qquad (4.17)$$

when

$$\bar{T}_h \geq \bar{T}_{h(HAZ)} \qquad \text{i.e.,} \qquad \phi \geq \phi_{HAZ} = \bar{T}_{h(HAZ)}/T_a \qquad (4.18)$$

(layer temperature reaches a hazardous value)

or

$$Z_i \leq Z_{i(HAZ)} \qquad \text{i.e.,} \qquad \zeta \leq \zeta_{HAZ} = Z_{i(HAZ)}/L_c \qquad (4.19)$$

(interface reaches a hazardous elevation)

From the computed history of ϕ and ζ, and compatible with the detection criterion which is invoked, the time of detection would be obtained. This would be defined as that time,

$$t_{DET} \qquad \text{i.e.,} \qquad \tau_{DET} = t_{DET}/t_c \qquad (4.20)$$

when e.g.,

$$H-Z_i \geq \Delta_{DET} \qquad \text{i.e.,} \qquad \zeta \leq \zeta_{DET} = (H-\Delta_{DET})/L_c \tag{4.21}$$

(layer thickness detection criterion)

and/or

$$\bar{T}_h \geq \bar{T}_{h(DET)} \qquad \text{i.e.,} \qquad \phi \geq \phi_{DET} = \bar{T}_{h(DET)}/T_a \tag{4.22}$$

(layer temperature detection criterion)

and/or

$$d\bar{T}_h/dt \geq (d\bar{T}_h/dt)_{DET} \qquad \text{i.e.,} \tag{4.23}$$

$$d\phi/d\zeta \geq (d\phi/d\tau)_{DET} = (t_c/T_a)(d\bar{T}_h/dt)_{DET}$$

(layer rate of temperature rise detection criterion)

The time of detection corresponding to other detection criteria which were similarly related to ϕ or ζ, etc. could also be obtained.

From all the above the desired value for safe available egress time,

$$t_{EG} \qquad \text{i.e.,} \qquad \tau_{EG} = t_{EG}/t_c \tag{4.24}$$

would be computed from

$$t_{EG}=t_{HAZ}-t_{DET} \qquad \text{i.e.,} \qquad \tau_{EG} = \tau_{HAZ} - \tau_{DET} \tag{4.25}$$

4.4 A Computer Program

A computer program was written to solve the problem outlined in the above paragraphs. The code accepts representations of $\dot{Q}$ in one of three possible forms, viz, digital data points with linear interpolation, digital data points with exponential interpolation, and analytic representation. Hazardous conditions are determined per Eqs. (4.18) and (4.19) where arbitrary choices for $Z_{i(HAZ)}$, and $\bar{T}_{h(HAZ)}$ can be made.

Detection criteria per Eqs. (4.21), (4.22) or (4.23) can be chosen where arbitrary choices for Δ_{DET}, $\bar{T}_{h(DET)}$, or $(d\bar{T}_h/dt)_{DET}$ can be assigned.

Safe available egress times for some example fire scenarios were obtained with the use of this computer code. The results of these computations are presented in the next section.

5. AVAILABLE EGRESS TIME FROM ROOMS OF FIRE ORIGIN - SOME EXAMPLE CALCULATIONS

5.1 An Introduction to Two Example Scenarios

This section presents results of the use of the quantitative model developed in the previous section. In particular the model has been used to investigate the available egress times that would result from fires in two different types of fuel assemblies.

One of the fuel assemblies that was studied was a particular mattress construction and adjacent igniting wastepaper basket whose combined free burn energy release had been previously determined from weight loss measurements. The development of the hazardous environment generated by this fuel assembly as it burned in a full scale hospital patient room-corridor mockup had also been observed experimentally. Data from this latter test were therefore available for the purpose of a partial evaluation of the model's general predictive capability.

A free burn in the second fuel assembly was assumed to release energy according to a composite semi-universal fire constructed from free burn data summarized in [1]. A set of calculations using this as the threatening fuel assembly was carried out. The results of these calculations are presented here for the purpose of providing a hint of the model's utility in presenting building designers with practical estimates of safe available egress time, e.g., when the fuel assemblies in the room or building of interest are (anticipated to be) characteristic of a given type of occupancy.

5.2 Assumptions on the Disposition of Energy Release and Their Implications

In order to use the model for any given free burn energy release data, values of λ_r and λ_c (the effective fraction of the energy release that is radiated out of the combustion zone, and the net fraction of $\dot{Q}(t)$ that is transferred to the room boundaries, respectively; c.f., section 4.2) are required. While appropriately chosen constant λ values should prove to be adequate for most engineering applications, the method described can, through specified dynamic variations in these λ's, readily accept more detailed characterizations of the gas-to-room surface heat transfer phenomena.

Depending on the fuel and its configuration Burgess and Hertzberg [18] and DeRis [19] report that the total radiant power output in fire combustion zones tend to fall in the range of 15-40 percent of the total rate of heat release. Based on this and, for example, on recent data presented by Modak and Croce [20] it appears that the use of a figure of $\lambda_r = .35$ in Eq. (4.2) is a reasonable choice for the type of growing hazardous fires under consideration. This value was used in all calculations to be described below.

Using the .35 value for λ_r and taking account of convective heat transfer considerations an appropriate value for λ_c was developed in Appendix A. This was found to lie in the approximate range 0.6 - 0.9. The lower, 0.6 value would relate to high aspect ratio spaces (ratio of ceiling span to room height) with smooth ceilings and with fires positioned far away from walls. The intermediate values and the high 0.9 value for λ_c would relate to low aspect ratio spaces, fire scenarios where the fire position is within a room height or so from walls, and/or to spaces with highly irregular ceiling surfaces. In the latter types of situations, which are representative of most realistic fire scenarios, it is not presently possibly to provide general rules to accurately estimate λ_c within this 0.6 - 0.9 range. This fact has especially strong implications on the capability for establishing accurate estimates

for the average upper layer temperature. This can be seen from the second of Eq. (4.8) where, early in the fire and at times of relatively cool upper layer temperatures (ϕ close to 1), $d\bar{T}_h/dt$ and, ultimately, $\bar{T}_h - T_a = \Delta\bar{T}_h$ are seen to be proportional (through the factor c_1) to $(1 - \lambda_c)$. In contrast to the upper layer temperature estimate and during the early growth stages of the fire, the upper layer - lower layer interface position history is not nearly as sensitive to inaccuracies in λ_c. At such early times $\dot{q}$ is of the order of 1 and ζ is close to H/L_c. A study of the first of Eq. (4.8) together with the c_1, c_2 values of Eq. (4.9) reveals that under such $\dot{q}$, ζ conditions the second term on the right side of Eq. (4.8), which is independent of λ_c, strongly dominates the first term.

The above discussion leads to the following guidelines for selection and use of a value for λ_c, when a reliable estimate of it's actual value is not otherwise available:

a. For the purpose of computing a conservative estimate of the time when a hazardous temperature or a hazardous interface elevation will be attained (i.e., the predicted t_{HAZ} will be less than the observed t_{HAZ}) one should select $\lambda_c = 0.6$.

b. For the purpose of a conservative estimate of detection time when detection is by temperature or rate of temperature rise of the upper layer (i.e., the predicted t_{DET} will be greater than the actual t_{DET}) one should select $\lambda_c = 0.9$.

c. When fire detection is by temperature or rate of temperature rise an accurate (as compared to a conservative) estimate of detection time is achievable only 1) in large aspect ratio, smooth ceiling spaces where detection is based on a $\lambda_c = 0.6$ computation of average upper layer temperature; and 2) in other configurations where detectors are deployed near the ceiling in some regular grid array and where the time of detection is based on estimates of actual ceiling jet temperature (i.e., predictions of average upper layer

temperature are not the basis determining likely times of detection). Such estimates are provided, for example, in references [8,9,11 and 13].

5.3 The First Scenario - An Indication of the Model's Predictive Capability

5.3.1 General Description of the Hospital Patient Room-Lobby Scenario

This section covers some comparisons between the results of a practical full scale fire experiment and calculations based on the concepts developed above. The actual experiment considered is one of a series of full scale tests of a mockup hospital patient room-corridor building space. The test series, described in detail by O'Neill and Hayes [21], was for the purpose of evaluating the utility of sprinkler systems in hospitals. The specific test run from that series which will be considered here does not involve sprinkler operation.

It is noteworthy that the test data that was acquired, although appropriate and adequate for the original test objective, only provides a minimal base for the comparisons that are of interest in the present work. Nevertheless, the experimental vs theoretical comparisons to follow verify, indeed extend, the utility of the ideas developed in this investigation.

A plan view of the building space is presented in Figure 8. The space is made up of a room of area 155 ft^2 (14.4 m^2) connected by an open doorway to a corridor-lobby configuration of area 800 ft^2 (74.3 m^2).

A fire is initiated in a wastepaper basket next to the corner of a polyurethane mattress covered with bedding. The wastepaper basket-mattress fuel assembly and its mode of ignition was carefully reproduced in most runs of the test series referred to above including the test run under present consideration. The burn characteristics of this assembly

were studied in detail prior to the room burns of this series [14]. The history of the energy release rate as derived from weight loss measurements is plotted in Figure 9. For the purpose of the present analysis it is assumed that this energy release rate was reproduced in the actual test run under review. However, some significant deviations from the Figure 9 energy release rates are a distinct possibility especially during the early growth stage of the fire, say, 0-100 seconds, during which time the wastepaper basket involvement dominates the fire development.

The model which has been quantitatively detailed in section 4 is a single room or room of fire origin model. Thus, it may not be immediately obvious at what point, if any, it will have relevance to the present fire scenario. Together with the general ideas of sections 1-3, it would appear that a two room or multi-room flow dynamics model of the type developed by Zukoski and Kubota [22] or Tanaka [23] would generally be required to study the room-corridor-lobby scenario under consideration. (For example, a two room example flow calculation for a set of fire and room size parameters which somewhat correspond to the present scenario has been considered in [22]). Nevertheless, it is possible that a simple, single room modeling approach to fire scenarios involving relatively free-flowing multi-space configurations can be adequate for the purpose of obtaining engineering estimates of available egress time in the range of conditions that occured in the referenced hospital patient room-corridor test.

5.3.2 The Room of Fire Origin

For early times into the fire, prior to the time when the layer interface drops to the level of the connecting doorway soffit, the single room model is completely relevant for the burn room. Up to that point the open doorway acts as the lower leakage path referenced in section 4.2. Using the energy release data of Figure 9, the model was therefore used to compute the POC filling history of a 155 ft^2 (14.4 m^2)

room up to the time that the layer thickness exceeded the existing ceiling to soffit dimension of 1.33 ft (.41m). A value of $\lambda_c = .72$ was used in Eqs. (4.8). This estimate for λ_c is based on a calculation which is presented in section A.3 of the appendix. In this calculation the contribution to convective heat transfer was taken from the reduced scale room fire studies of Zukoski and Kubota [24]. The contribution to radiative heat transfer was taken to be consistent with the $\lambda_r = .35$ value discussed in section 5.2. The time for the interface to reach the soffit was computed to be 21 seconds following ignition.

5.3.3 The Adjacent Space

Once the smoke flows under the soffit and starts to fill the large corridor-lobby space, a two room model is required to describe the gas migration and exchange between the two spaces. This would continue to be true for at least some intermediate time interval. Following this, the single room model can again be relevant as discussed below.

If the fire is small enough or the doorway is large enough so that flows through the doorway remain relatively weak the adjacent space will eventually attain and maintain a smoke layer thickness essentially identical to that of the burn room. After some time interval the histories of the elevations of the layer interfaces in both spaces will be similar and can be computed from a single room model, where the single room has an area equal to the combined area of both spaces. Time intervals when the upper layer thicknesses of the two rooms are <u>not</u> similar would encompass 1) the initial time when the room of origin fills up with smoke to the level of the doorway soffit, and 2) the subsequent time interval when the upper layer thickness of the adjacent space grows from zero to a value close to that of the room of fire origin.

For fire scenarios where the above is applicable, significant simplifications occur in that the relatively simple single room of fire origin model can be used to study the significant effects of fire growth

when far more complicated multi-room models would, at first hand, appear to be required.

In an attempt to test the utility of the above ideas the single room model was used to predict the history of a single interface elevation and the average upper layer temperature within the combined patient room-corridor space. Using the energy release rate of Figure 9 and a total room area of 955 ft^2 (88.7 m^2) the history of the interface elevation and of the average upper layer temperature was computed. An effective λ_c for this combined space scenario is expected to be greater than the above $\lambda_c = .72$ value used for the single room of fire origin. This is the case because of the additional heat transfer to the corridor surfaces. A value of $\lambda_c = .85$ was selected for the calculation. This was done with the anticipation that comparisons between computed and experimental average upper layer temperatures would reveal an appropriate correction to this λ_c value. (Recall from section 5.2 that the upper layer temperature difference, $\Delta\bar{T}_h - T_a$, is approximately proportional to $1 - \lambda_c$). The results of the computation for interface position and layer temperature are presented in Figures 10 and 11 respectively.

For the purpose of comparing results for the analytic and experimental interface position an operational definition of the experimental interface position was required. This definition was based on the outputs of a total of 6 photometers placed at three different elevations and at one to three different positions (indicated in Figure 8) in the corridor and lobby. The measured optical density (OD) outputs of these photometers are indicated in Figure 12. From these latter outputs, and for the purpose of defining a time when the smoke layer interface position passes the elevations of these photometers, there is still ambiguity as to what value of OD should constitute the presence of a smoke layer. Four different OD values .01, .02, .03, and .04 were used as possible definitions for a minimum upper layer OD. Using the photometer outputs, the result of these four possible interface definitions leads to four possible sets of experimental data points for the interface elevation vs time. These are plotted in Figure 10 together with

the theoretical results of the interface motion.

The agreement between the results of theoretical and experimental interface position at the lower two of the three photometer locations illustrates the capability of the model in the present instance to predict the growth of the potentially hazardous upper smoke layer thickness. As discussed earlier, a favorable comparison at the uppermost photometer elevation located .20 ft (.06 m) from the ceiling was not to be expected. This is because of the fact that in the present multispace configuration the single room model implemented in the manner described is clearly not adequate to predict the early layer growth in the corridor-lobby portion of the test space.

Gas temperatures were measured by two thermocouple trees located in the center of the corridor 15 ft (4.6 m) on either side of the burn room doorway. No temperature data was acquired in the lobby space. At any given time the equi-level thermocouples of these two trees measured temperature differences, $T-T_a$ which agreed to within 20 percent of one another. For the purpose of comparing analytic and experimental average layer temperature histories an appropriate instantaneous weighting of the measured temperatures of the limited number of these corridor thermocouples was required. At a given instant of time this weighting had to be consistent with the estimate/ measurement of the interface position as well as the relative position of the thermocouples in question. A plot of the measured average layer temperature history deduced from such a data reduction scheme is presented along with the plot of the computed temperature history in Figure 11. As noted earlier, if a different λ_c had been used in the computation then, to a first approximation (i.e., using the "principle of proportionality" between $\Delta\bar{T}_h$ and $1-\lambda_c$), one would anticipate a shift from the originally computed $\Delta\bar{T}_h(t)$ (with $\lambda_c = .85$) to a new temperature history, $\Delta\bar{T}_h^{(new)}(t)$ (with $\lambda_c = \lambda_c^{(new)}$), where

$$\Delta\bar{T}_h^{(new)}(t) = [(1 - \lambda_c^{(new)})/(1 - .85)]\ \Delta\bar{T}_h(t) \qquad (5.1)$$

In view of the above it is possible to bring the predicted analytic $\bar{T}_h$ plot into coincidence with the experimental $\bar{T}_h$ plot for at least one instant of time by a new choice, $\lambda_c^{(new)}$, for λ_c. Such coincidence is attained at t = 330 seconds [when the computed layer interface is at the potentially hazardous position 3 ft (.91 m) from the corridor floor] by the specific choice of $\lambda_c^{(new)} = 0.947$. Using this latter value of $\lambda_c^{(new)}$ in Eq. (5.1) an adjusted average upper layer temperature history was computed and plotted in Figure 11.

The single room model was also used to recompute the interface position and temperature histories corresponding to $\lambda_c = .947$. These are plotted in Figures 10 and 11, respectively. For the parameters of the present scenario, the proximity of the $\lambda_c = .85$ and $\lambda_c = .947$ plots of Figure 10 illustrates the relative insensitivity of the interface position history to changes in λ_c. The variations between the two $\lambda_c = .947$ temperature history estimates are so small that they cannot be discerned in Figure 11. For this scenario this fact illustrates the validity of the "principle of proportionality" as expressed through Eq. (5.1).

As can be noted in Figure 11, the overall comparison between the experimental and newly calculated estimates for the upper layer temperature history is good in the time interval 175-330 seconds but poor at earlier times. One would hope that these temperature comparisons would be favorable for a longer time interval if the spatial distribution of the corridor thermocouples had been more refined, i.e., if a more accurate estimate of experimentally determined average upper layer temperature was available. It is possible, however, that the relatively complicated nature of the energy transfers which are being simulated may preclude sharper estimates of $\bar{T}_h$ with the use of a single, constant value of λ_c. Also, as noted earlier, the single room simulation of the multi-room flow dynamics must inevitably break down during some initial interval.

5.4 Available Egress Time in a Semi-Universal Fire

If the present concept on estimating egress time is to have utility to practitioners of fire safety it will be necessary that the significant elements of potentially threatening fire scenarios be identified. It will also be necessary for the results of egress time analyses to be presented in a concise and practical manner. This paragraph provides an example of how the whole concept might proceed in practice.

First, one must deal with quantitative characteristics of a particular, potentially threatening, free burn fire of concern. Paragraph 2.3 dealt with some practical considerations that would be useful in deducing such characteristics. For the present purpose a composite, semi-universal type fire has been constructed from the data of Table 1. The fire's energy release history is plotted in Figure 13. The fire is assumed to be initiated from a 10 kW (9.5 BTU/sec) ignition source. Initially, it grows exponentially at a growth rate which is characteristic of a fire initiated in a polyurethane mattress with bedding. This early growth rate would be characteristic of the early growth of threatening fires in a variety of occupancies which typically contain upholstered polyurethane cushioning, e.g., hospital patient and lobby rooms, residential spaces and auditoriums. From Table 1, it would also appear to be consistent with the (unreported) early growth stage of fires in large assemblies of commodities stacked on pallets. Beyond 400 kW (380 BTU/sec) and consistent with Table 1, the fire of Figure 13 is assumed to grow at a rate which is similar to and/or which bounds the anticipated growth of fires initiated in a variety of different types of commodities stacked on pallets. This latter portion of the semi-universal fire is no doubt also representative of other threatening fires in large merchantile and/or business occupancies.

The fire of Figure 13 was assumed to be initiated in a variety of different size spaces. The geometries of these spaces are characterized by areas ranging from 300-10,000 ft^2 (28-929 m^2) and by heights ranging from 8-20 ft (2.4 - 6.1 m).

Various possible criteria for fire detection were considered in the analysis of available egress time. These included instantaneous detection (by whatever means), i.e., at a time when the upper hot layer thickness $\Delta Z_{DET} = 0$; detection by smoke detectors which is assumed to occur at a time when ΔZ_{DET} = 1 ft = .3 m, and detection when the upper gas layer reaches an average temperature of 135°F (54°C)*. As noted at the end of section 3.4, the utility of the latter two detection criteria are at present strictly speculative. They are included here only to illustrate the type of results which one might hope to generate by applying the methodology under discussion.

The criterion for the onset of hazardous conditions is an upper layer interface position 3 ft (.91 m) above the floor, or an average upper layer temperature of 361°F (183°C) (corresponding to .25 W/cm^2), whichever comes first.

It is assumed that 35 percent of the fire's instantaneous energy release rate is radiated from the combustion zone (λ_r = .35) and that a total of 60 percent of this energy release rate is transfered to the surfaces of the room and it's contents, i.e., 40 percent of this energy is retained in the upper layer products of combustion (λ_c = .60). Recall that the latter choice of λ_c would be appropriate for large aspect ratio spaces with smooth ceilings, but, in any event the choice of λ_c would have a minor impact on estimated egress times in cases where criteria of detection or hazard are not dependent on upper layer gas temperature.

With the above range of parameters the quantitative particulars of section 4 were used to compute estimates for available egress times. The results of these computations are presented in Figure 14. In that figure, available egress time ($t_{HAZ} - t_{DET}$) is plotted as a function of

---

* The technology now exists to produce a temperature sensitive detection device which would respond in a manner consistent with this detection criterion [25].

room area for different parametric values of room height and for different detection criteria.

As an example of the utility of Figure 14 consider a scenario where a fire is initiated in an occupied, 5,000 ft^2 (465 m^2) nominal 20 ft (6.1 m) high ceiling auditorium outfitted with polyurethane cushion seats (which are assumed to be the most significant fuel load). Then, from Figure 14 one would estimate an available egress time of approximately seven minutes. This assumes immediate detection as a result of occupant recognition and verbal alarm to fellow occupants at the time of fire initiation. If the auditorium is to be considered safe relative to successful egress, then a further study would have to reveal that the time required for a capacity crowd to evacuate the auditorium is less than these seven minutes.

The following general features of the results of Figure 14 are noteworthy:

a) As is well known, for life safety as it relates to safe egress, temperature detectors are far less effective than smoke detectors.

b) For a given curve, moving up in room area eventually leads to an abrupt reduction in the curve's slope. This is the result of a shift in the triggering mechanism for onset of hazardous conditions. On the left side of the change in slope (smaller areas), untenability occurs as a result of the layer interface dropping to the 3 ft (.91 m) level. On the right side (larger areas), untenability occurs as a result of thermal radiation from a hot upper layer.

c) For some curves [e.g., 8 ft (2.4 m) ceiling height, Δ_{DET} = 1 ft (.3 m)] the available egress time actually decreases with increasing area for areas in excess of some critical area. This occurs because the specified Figure 13 fire will take a

longer time (t_{DET}) to fill a larger area room to a given specified upper layer thickness (Δ_{DET}). But, the longer this time of detection, the higher will be the upper layer temperature at the time of detection. Accordingly, with increasing area a diminishing amount of egress time is available beyond t_{DET} before the hazardous upper layer temperature T_{HAZ} is achieved. Beyond some (large) area this phenomenon of shrinking available egress time with larger area will not represent a realistic sequence of events. For example, the phenomenon would break down when, say, detection by inevitable human response to high, but not yet hazardous, upper layer radiation occurs prior to the buildup of upper layer thickness to the specified Δ_{DET}.

6. SUMMARY, CONCLUSIONS AND FUTURE DIRECTIONS

6.1 Summary

The introductory section to this work presented the concept of attaining life safety in fires by means of safe egress. The concept involves two basic elements, namely, the time available for safe egress, t_{avail} (i.e., the time between fire detection and the onset of hazardous conditions), and the time required for safe egress, t_{req} (i.e., the time required for occupants to evacuate a threatened space). A safe condition would be indicated if $t_{avail} \geq t_{req}$. General ideas on estimating safe available egress time from rooms of fire origin and from adjacent spaces were discussed. Actual estimates would be based on a model of the development of hazardous conditions in a specified space subsequent to the initiation of a specific fire. Appropriate criteria for both fire detection and onset of untenability would be used to identify these two events within the simulated time-varying-description of the degrading environmental conditions.

Relative to the task of estimating available egress time, Section 2 was devoted to a discussion of the significance and utility of free burn

testing of practical fuel assemblies. Such tests would be carried out on fuel assemblies which are characteristically found in different occupancies. The data from the tests would be used as inputs to the safe available egress time estimation scheme.

By introducing a definite qualitative and quantitative model of hazard development, the details of an available egress time estimation technique were formulated in Sections 3 and 4 for the room of fire origin problem. The model basically assumes that the products of combustion rise in a plume which forms above a threatening fire, and that these products fill the room from above with a hot, potentially toxic, obscuring, and ever-thickening smoke layer.

In Section 5 the room of fire origin model was used in two example problems. First, results from the model were compared to actual test data which were generated in a full scale test of a hospital patient room-corridor mockup fire scenario. Favorable comparisons between the computed and measured evolution of the upper layer depth suggest that for some practical problems the use of the (single) room of fire origin model can be extended to freely connected multiple space configurations. Comparisons between computed and measured results also suggested that the limited nature of available estimates in overall heat transfer to ceilings and walls can lead to serious errors in estimates of average upper layer temperature.

The second example problem of Section 5 presented a hint of the ability of the room of fire origin egress model, indeed, of the overall egress concept, to provide building designers with practical estimates of available egress time. There, a hybrid, semi-universal fire (Figure 13) was analytically constructed from data acquired in diverse, practical fuel assembly free burns. Rooms of different areas and heights were assumed to contain this fictitious fire, and for a specific realistic hazard criterion, available egress times were estimated for different detection criteria.

6.2 Conclusions and Future Directions

From the above it is concluded that the concept of achieving life safety in fires through safe egress is not only qualitatively useful, but it can be quantitatively applied to real building problems by means of practical and rational engineering calculations. This work has suggested general ideas on formulating the essential elements of a physical fire development model that would be the basis for such calculations. These elements would be constructed from a variety of well established, experimentally and theoretically derived enclosure fire phenomena.

Fire growth models that are developed to provide fire protection practitioners with available egress time estimates are likely to represent compromises between accuracy in simulation and practicality in implementation. With regard to "optimizing" such compromises in the specific model adopted here, somewhat more modeling detail can readily be brought into play without seriously detracting from the model's practicality. For example, it is anticipated that near term future embellishments of the room of fire origin model will include dynamic estimates of product of combustion concentrations in the upper layer. This capability would allow both detection and untenability to be realistically based on such concentrations.

Room of fire origin results were shown to have some applicability to freely communicating, multiple space fire scenarios. However, the application of such results to multiple space problems is not generally appropriate. Accordingly, there is a clear requirement to develop a practical, generalized technique to solve the (available egress time from) adjacent space egress problem, and utlimately, to solve the overall building egress problem. This work has outlined guidelines for such solution techniques. The major new directions for future work on the available egress time problem clearly lie in the implementation of these guidelines.

7. ACKNOWLEDGEMENTS

Throughout the entire course of this work the author received the enthusiastic support of Mr. Harold Nelson who, while helping to provide a stimulating environment on a regular basis, freely shared his vast experience and keen insight into fire safety engineering technology, in general, and fire protection engineering, in particular.

Most calculations reported in this work were performed by Mr. Steven West who took the original room-of-fire-origin computer program and revised it in a manner as to significantly increase its versatility.

All of the above is gratefully acknowledged.

8. REFERENCES

[1] Friedman, R., Quantification of Threat from a Rapidly Growing Fire in Terms of Relative Material Properties, Fire and Materials, Vol. 2, No. 1, 1978.

[2] Emmons, H.W., Mitler, H.E., and Trefethen, L.N., Computer Fire Code III, Home Fire Project Tech. Rpt., No. 25, Div. Appl. Sciences, Harvard Univ., Jan., 1978.

[3] Cooper, L.Y., The Measurement of Smoke Leakage of Door Assemblies During Standard Fire Exposures, NBSIR 80-2004, U.S. Dept. Commerce, Nat'l. Bur. Standards, Center for Fire Research, June, 1980.

[4] Pape, R., Mavec, J., Kalkbrenner, D., and Waterman, T., Semistochastic Approach to Predicting the Development of a Fire in a Room from Ignition to Flashover. Program Documentation and User's Guide, Ill. Inst. Tech. Research Inst. Report NBS-GCR-77-111 prepared for U.S. Dept. Commerce, Nat'l. Bur. Standards, 1977.

[5] Baines, W.D. and Turner, J.S., Turbulent Buoyant Convection from a Source in a Confined Region, Journal Fluid Mech., Vol. 37, Part I, 1969.

[6] Zukoski, E.E., Development of a Stratified Ceiling Layer in the Early Stages of a Closed-Room Fire, Fire and Materials, Vol. 2, No. 2, 1978.

[7] Alpert, R.L., Turbulent Ceiling Jet Induced by Large Scale Fires, Tech. Report FMRC 22347-2, Factory Mutual Research Corp., 1974.

[8] Benjamin, I., Heskestad, G., Bright, R., Hayes, T., An Analysis of the Report on Environments of Fire Detectors, Fire Detection Institute, 1979.

[9] Alpert, R.L., Calculation of Response Time of Ceiling-Mounted Fire Detectors, Fire Technology, Vol. 3, 1972.

[10] Heskestad, G., and Delichatsios, M.A., Environments of Fire Detectors - Phase I: Effect of Fire Size, Ceiling Height, and Materials, Volume 1. Measurements, Factory Mutual Research Corp. Report NBS-GCR-77-86 prepared for U.S. Dept. Commerce, Nat'l. Bur. Standards, 1977.

[11] Heskestad, G., and Delichatsios, M.A., Environments of Fire Detectors - Phase I: Effect of Fire Size, Ceiling Heights, and Material. Volume 2. Analysis, Factory Mutual Research Corp. Report NBS-GCR-77-95 prepared for U.S. Dept. Commerce, Nat'l. Bur. Standards, 1977.

[12] Heskestad, G., and Delichatsios, M.A., Environments of Fire Detectors - Phase II: Effect of Ceiling Configuration. Volume I. Measurements, Factory Mutual Research Corp. Report NBS-GCR-78-128 prepared for U.S. Dept. Commerce, Nat'l. Bur. Standards, 1978.

[13] Heskestad, G., and Delichatsios, M.A., Environments of Fire Detectors - Phase II: Effect of Ceiling Configuration. Volume II. Analysis, Factory Mutual Research Corp. Report NBS-GCR-78-129 prepared for U.S. Dept. Commerce, Nat'l. Bur. Standards, 1978.

[14] Babrauskas, V., Combustion of Mattresses Exposed to Flaming Ignition Sources. Part I. Full-Scale Tests and Hazard Analysis, Center for Fire Research, NBSIR 77-1290, U.S. Dept. Commerce, Nat'l. Bur. Standards, 1977.

[15] Morton, B.R., The Choice of Conservation Equations for Plume Models, Journal Geophysical Research, Vol. 76, No. 30, 1971.

[16] Yokoi, S., On the Heights of Flames from Burning Cribs, BRI Report 12, Ministry of Construction, Japanese Government, 1963.

[17] Zukoski, E.E., Kubota, T., Cetegen, B., Entrainment in Fire Plumes, Calif. Inst. of Tech. Report supported through Grant No. G8-9014 of U.S. Dept. Commerce, Nat'l. Bur. Standards, April, 1980.

[18] Burgess, D., and Hertzberg, M., Radiation from Pool Fires, Chapter 27 of Heat Transfer in Flames, Afgan, N.H., and Beer, J.M., Eds., Wiley, 1974.

[19] DeRis, J., Fire Radiation - A Review, Tech. Report FMRC RC 78-BT-27, Factory Mutual Research Corp., 1978.

[20] Modok, A.T., and Croce, P.A., Plastic Pool Fires, Combustion and Flame, Vol. 30, 1977.

[21] O'Neill, J.G., and Hayes, W.D., Full-Scale Fire Tests with Automatic Sprinklers in a Patient Room, Center for Fire Research, NBSIR 79-1749, U.S. Dept. Commerce, Nat'l. Bur. Standards, 1979.

[22] Zukoski, E.E., and Kubota, T., A Computer Model for Fluid Dynamic Aspects of a Transient Fire In a Two Room Structure (Second Edition), Calif. Inst. Tech. Report prepared for U.S. Dept. Commerce, Nat'l. Bur. Standards, 1978.

[23] Tanaka, T., A Model on Fire Spread in Small Scale Building, Third Joint Meeting U.S.-Japan Panel on Fire Research and Safety, U.J.N.R., Wash., D.C., March 13-17, 1978.

[24] Zukoski, E.E., Kubota, T., An Experimental Investigation of the Heat Transfer from a Buoyant Plume to a Horizontal Ceiling - Part 2. Effects of Ceiling Layer, Calif. Inst. of Tech. Report NBS-GCR-77-98 prepared for U.S. Dept. Commerce, Nat'l. Bur. Standards, 1975.

[25] Bukowski, R., private communication.

[26] Veldman, C.C., Kubota, T. and Zukoski, E.E., An Experimental Investigation of the Heat Transfer from a Buoyant Gas Plume to a Horizontal Ceiling - Part 1. Unobstructed Ceiling, Calif. Inst. Tech. Report NBS-GCR-77-97 prepared for U.S. Dept. Commerce, Nat'l. Bur. Standards, 1975.

[27] Cooper, L.Y. and O'Neill, J.G., Fire Tests of Stairwell Sprinkler Systems to Appear as Center for Fire Research NBSIR, U.S. Dept. Commerce, Nat'l. Bur. Standards.

APPENDIX A. HEAT TRANSFER TO THE BOUNDING SURFACES OF THE ROOM OF FIRE ORIGIN

A.1 Introduction

This appendix is for the purpose of establishing an appropriate value for λ_c to use in Eqs. (4.8). As noted in section 4.2, λ_c is defined as the combined instantaneous fraction of $\dot{Q}$ lost by the combustion zone, the plume gases, and the hot upper layer gases to the bounding surfaces of the room and it's contents. λ_c is made up of radiation losses and convection losses.

As discussed in section 5.2, for the present purposes it is reasonable to assume that 35 percent of the fire's energy release rate, $\dot{Q}(t)$, is radiated from the combustion zone. During the relatively early times under consideration here when exposed surfaces are still relatively cool, of the order of half of this energy "shines" on and is absorbed by the floor and by surfaces of furniture, hardware, etc., contained within the room. The remaining half of this $.35\ \dot{Q}$ irradiates the upper portions of the room. At very early times when the upper layer is relatively transparent because of it's small thickness and/or optical density, most of this upper radiant energy is actually absorbed by the ceiling. Somewhat later, a significant portion of this $.35\ \dot{Q}/2$ energy delivery may be trapped by the upper gas layer because of it's growing effective absorbtivity. With regard to energy transfer from the upper layer itself, it is reasonable to assume that for the times of interest here convective losses will dominate those energy losses which are due to upper layer reradiation. This latter assumption along with the above transparent upper layer assumption will be made below. To complete the picture and to eventually draw all the pieces together and finally select an appropriate effective λ_c, it is necessary to estimate the magnitude of the convective losses.

A.2 Convective Heat Transfer to the Ceiling

Assuming rooms with smooth surface, characteristic ceiling spans of the order of several room heights and with fires away from the walls, the losses from the upper layer to the ceiling will be the result of convection heat transfer from an axisymmetric ceiling jet. Alpert [7] has studied the ceiling jet problem both analytically and experimentally for the case of a constant fire size and for zero upper layer thickness. Veldman, Kubota and Zukoski [26] have added more experimental data to the heat transfer aspects of the problem. Zukoski and Kubota [24] have studied the heat transfer problem experimentally for configurations having upper layer thicknesses which grow to fixed values in the steady state. The latter work concluded that the heat transfer coefficients, h, for both the zero layer and finite layer thickness cases are substantially similar. The following correlates the heat transfer coefficient data of [26]

$$h/[\rho_\infty C_p (gH)^{1/2} (\dot{Q}^*)^{1/3}]$$

$$= f_h = \begin{cases} 0.070(1-2.39\ r/H); & 0 \leq r/h \leq 0.2 \\ 0.0124(r/H)^{-0.67}; & 0.2 < r/H \leq 0.72 \end{cases} \qquad \text{(A-1)}$$

Here the rate of heat transfer to the ceiling, u, is defined as

$$u = h[T_{ad} - T_c] \qquad \text{(A-2)}$$

where T_{ad} is the near-ceiling jet temperature for an adiabatic ceiling, and T_c is the ceiling temperature.

An analytic estimate of the effective ceiling jet temperature, T_{ad}, in the zero layer thickness case which fits the data of [26] is given by

$$(T_{ad} - T_a)/[T_a (\dot{Q}^*)^{2/3}]$$

$$= f_t = 10.2 \exp(-1.77\ r/H); \quad 0 \leq r/H \leq 0.72 \qquad \text{(A-3)}$$

In the case of a finite layer thickness the plotted results of Figure 11 of [24] indicate that the values of T_{ad} will be larger than indicated by the above equation. This is due to the fact that instead of entraining ambient air the plume entrains heated gases of the upper layer once it passes through the upper layer-lower layer interface. In terms of actual data, the enhanced T_{ad} measurements of [24] for the finite layer are peculiar to the particular configurations used in that study. As it turns out, a general expression for T_{ad}, say as a function of Z_i/H, fire size, room aspect ratio (charcteristic ceiling span divided by H), and room lining materials, is not yet available. Since the zero layer result of Eq. (A-3) will be valid for early times and possible for later times in the case of rapidly growing fires (where, at a given instant, plume temperatures will tend to be significantly larger than the average upper layer temperature), it is reasonable to use it in the present calculations.

Using the above ideas together with the results of Eqs. (A-1) and (A-3) in Eq. (A-2), the rate of heat transfer can be computed from

$$u(r/H) = \rho_a C_p T_a (gH)^{1/2} \dot{Q}^* f_h [f_T - (T_c/T_a - 1)/(\dot{Q}^*)^{2/3}]$$

where f_h, f_T and T_c are all functions of r/H. The convective heat transfer to the ceiling, $\dot{Q}_{ceiling}$, within a circle of radius r can be computed from

$$\dot{Q}_{ceiling} = 2\pi H^2 \int_o^{r/H} u(\xi)\xi d\xi$$

or, using the above result for u and the definition of $\dot{Q}^*$ [below Eq. (4.2)],

$$\dot{Q}_{ceiling}/\dot{Q} = \lambda_{ceiling}(r/H)$$

$$= 2\pi(1-\lambda_r)\int_o^{r/H} f_h(\xi)\{f_T(\xi)-(T_c/T_a-1)/(\dot{Q}^*)^{2/3}\}\xi d\xi$$

For the present problem it will be assumed that the ceiling temperature has not increased significantly above an initial T_a value in the relatively short times of interest. Thus

$$\dot{Q}_{ceiling}/\dot{Q} = \lambda_{ceiling}(r/H) = 2\pi(1-\lambda_r)\int_o^{r/H} f_h(\xi)f_T(\xi)\xi d\xi \qquad (A-4)$$

Using the analytic expressions of Eqs. (A-1) and (A-3), and assuming that the validity of these equations can be extended up to r/H = 2, the value of $\lambda_{ceiling}(r/H)/(1-\lambda_r)$ in the range $0 \leq r/H \leq 2$. has been computed from a numerical integration of Eq. (A-4). The results of this is presented in Figure 15.

As seen in Figure 15, $\lambda_{ceiling}/(1-\lambda_r)$ appears to be approaching a large r/H asymptotic value of approximately 0.40. In view of the earlier $\lambda_r = .35$ estimate, it is therefore concluded that for rooms with ceiling spans of the order of 4H or larger the convective heat transfer to the ceiling can be estimated from

$$\lambda_{ceiling}(r/H>2) \simeq 0.40\ (1-\lambda_r) = .40\ (1 - .35) = .26$$

For rooms of smaller ceiling spans, appropriate smaller values of $\lambda_{ceiling}$ can be estimated with the use of the results of Figure 15.

A.3 Constructing a Value for λ_c

It is important to note that the above estimate for $\lambda_{ceiling}$ does not account for convective heat transfer to ceilings with deep surface irregularities (e.g., greater than .02H in depth). Nor does this estimate account for variations in ceiling heat transfer that come about as a result of strong ceiling jet-wall interactions which can occur in the vicinity of ceiling-wall junctions. It is also apparent that the above result does not take account of heat transfer to wall surfaces themselves. The total amount of all of these potential variations in convective heat transfer rates can be a significant fraction of $\dot{Q}$. This would be

particularly true in a scenario where (1) the fire is close enough to a wall so that strong flow interactions occur between the ceiling jet and the wall (this would always occur in rooms with span to height ratios smaller than 2-4) or (2) the ceiling has deep irregularities (e.g., deep beams) which are generally closer together than 2H - 4H.

Define the rate of convective heat transfer over and above $\dot{Q}_{ceiling}$ [defined in Eq. (A-4)] as $\dot{Q}_{other}$.

Now in a room with a smooth ceiling where the fire distance from the wall is several multiples of H or greater the value of $\lambda_{other} = \dot{Q}_{other}/\dot{Q}$ may be negligible compared to $\lambda_{ceiling} \simeq .40(1-\lambda_r)$. For such scenarios,

$$\lambda_c \simeq \lambda_r + \lambda_{ceiling} + \lambda_{other} \simeq .35 + .26 + \lambda_{other} \simeq 0.6$$

On the other hand, where $\dot{Q}_{other}$ or λ_{other} is significant, the total value of λ_c can be as large as 0.9. For example, in a series of large scale experiments reported by Cooper and O'Neill in [27] (1.5 and 4.0 MW propane diffusion flames in 3.7 m high space with deep ceiling beams and an aspect ratio of the order of two) λ_c was measured to be in the range .74 - .89. Also, in the small scale circular room experiments (.58 m high and .91 m in diameter) reported in [24], where radiation loss from a premixed propane burner (1.17 and 1.53 kW) was measured to be negligible [26], $(\lambda_{ceiling} + \lambda_{other})/(1 - \lambda_r)$ was estimated to be .57. It is noteworthy that data from these latter experiments were taken in the steady state. It is likely that a number larger than .57 would have been observed at early times into the experiments when ceiling and wall surfaces were near the original ambient temperature and when the energy content of the growing upper layer was increasing. For the large threatening fires of interest here where $\lambda_r = .35$ is assumed and where the other considerations of paragraph A.1 were valid, the above .57 value for $(\lambda_{ceiling} + \lambda_{other})/(1 - \lambda_r)$ leads to $\lambda_c = .72$.

A.4 Summary

To summarize all the above: λ_c for fire scenarios of interest here will generally fall within the approximate range

$$0.6 \leq \lambda_c \leq 0.9$$

The lower, 0.6 value would relate to high aspect ratio spaces with smooth ceilings and with fires positioned far away from walls. The intermediate values and the high 0.9 value for λ_c would relate to low aspect ratio spaces, fire scenarios where the fire position is within a room height or so from walls and/or to spaces with highly irregular ceiling surfaces.

Table 1. Various Factory Mutual Research Corporation fire data fitted to the exponential growth lay (from Friedman [1]): $\dot{Q} = \dot{Q}_1 \exp [\alpha(t-t_1)]$.

Fire Description	Range of Fire Size Fitted (kW)	$\alpha(sec^{-1})$	Doubling Time $0.693/\alpha$ (sec)
1. flex. PU foam 0.6 m x 0.6 m x 0.1 m high, ignited at top center	1 - 20	0.033	21
2. NSF bedroom fire 1975, PU mattress covered with sheet on bed in 8' x 12' room	10 - 400	0.024	29
3. wood crib, 0.76 m square, 0.38 m high, made of 120 pine sticks 3.2 cm. square, ignited at bottom center	150 - 1,000	0.018	38
4. Commodities on pallets in array 2.4 m x 2.6 m x 4.6 m high, ignited at bottom:			
a. paper cartons with metal liners	4,000 - 18,000	0.0029	240
b. toy parts in cartons	2,500 - 15,000	0.0040	170
c. polypropylene tubs in cartons	1,500 - 22,000	0.0045	150
d. compartmented paper cartons, empty	7,000 - 20,000	0.0057	120
e. air-cond. units on polyethylene pallets	2,000 - 40,000	0.0088	79
f. polystyrene meat trays, paper-wrapped	3,000 - 60,000	0.025	28
g. polystyrene insulation boards	7,000 - 100,000	0.029	24

Characteristic fuel assembly for ("Type A") offices

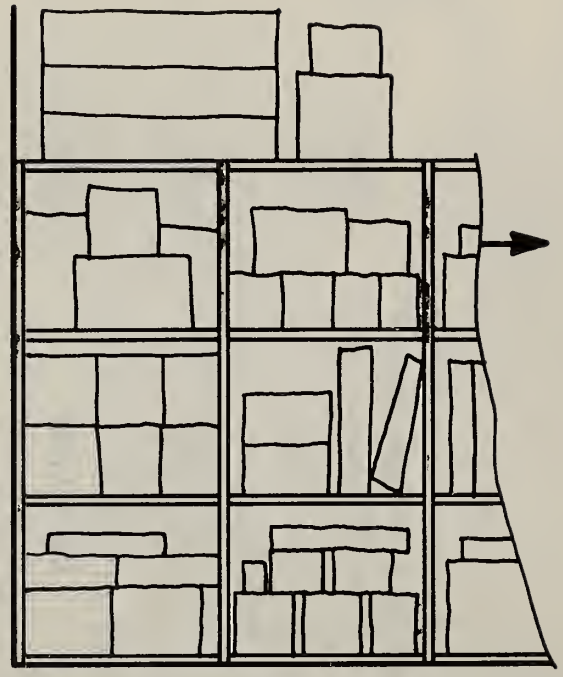

Characteristic fuel assembly for ("Type A") warehouses

Figure 1. Two examples of characteristic fuel assemblies of interest

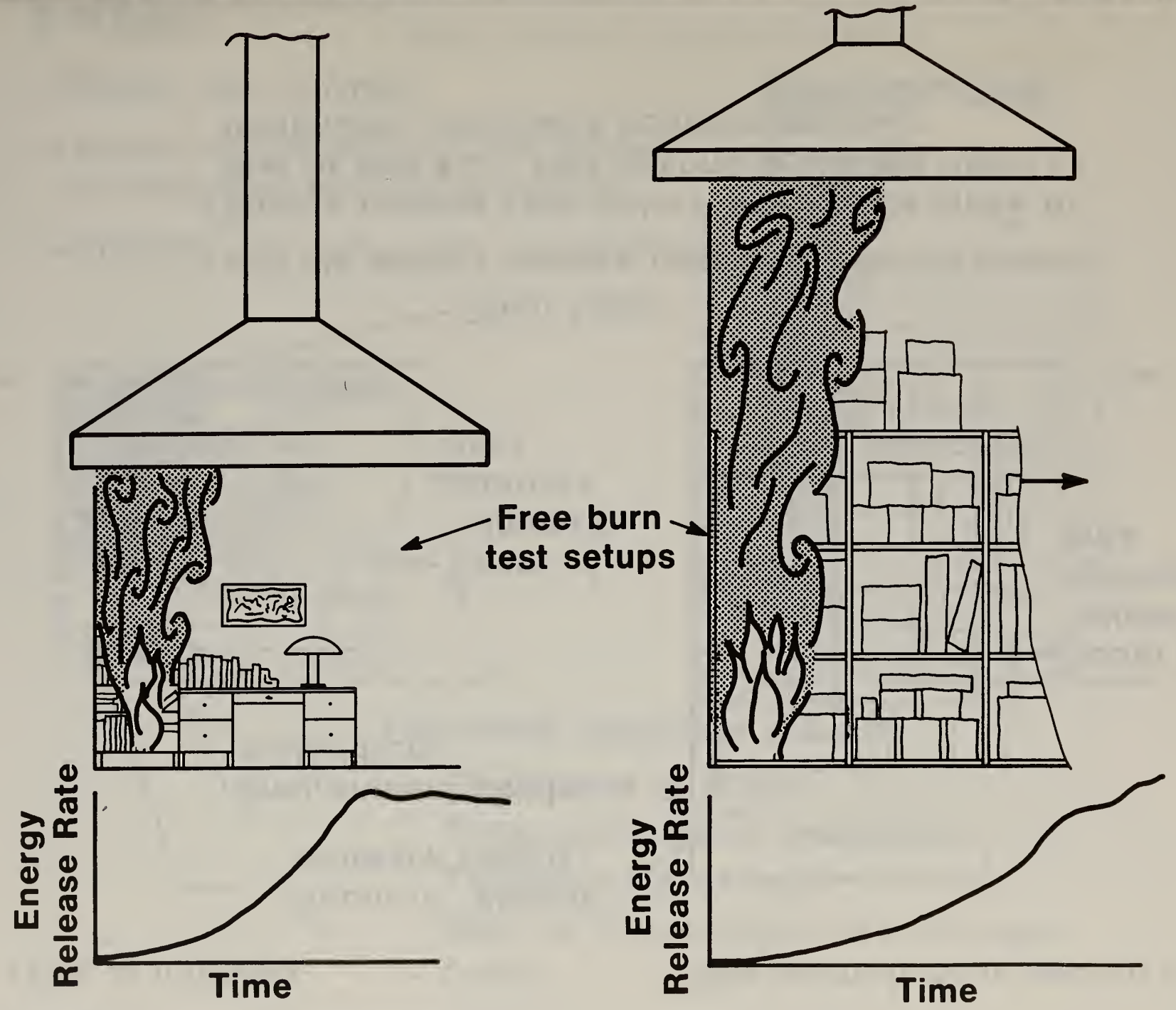

Figure 2. History of the energy release rate from free burn experiments

t = 0

- Fire is initiated

* See restrictions in section 3.2

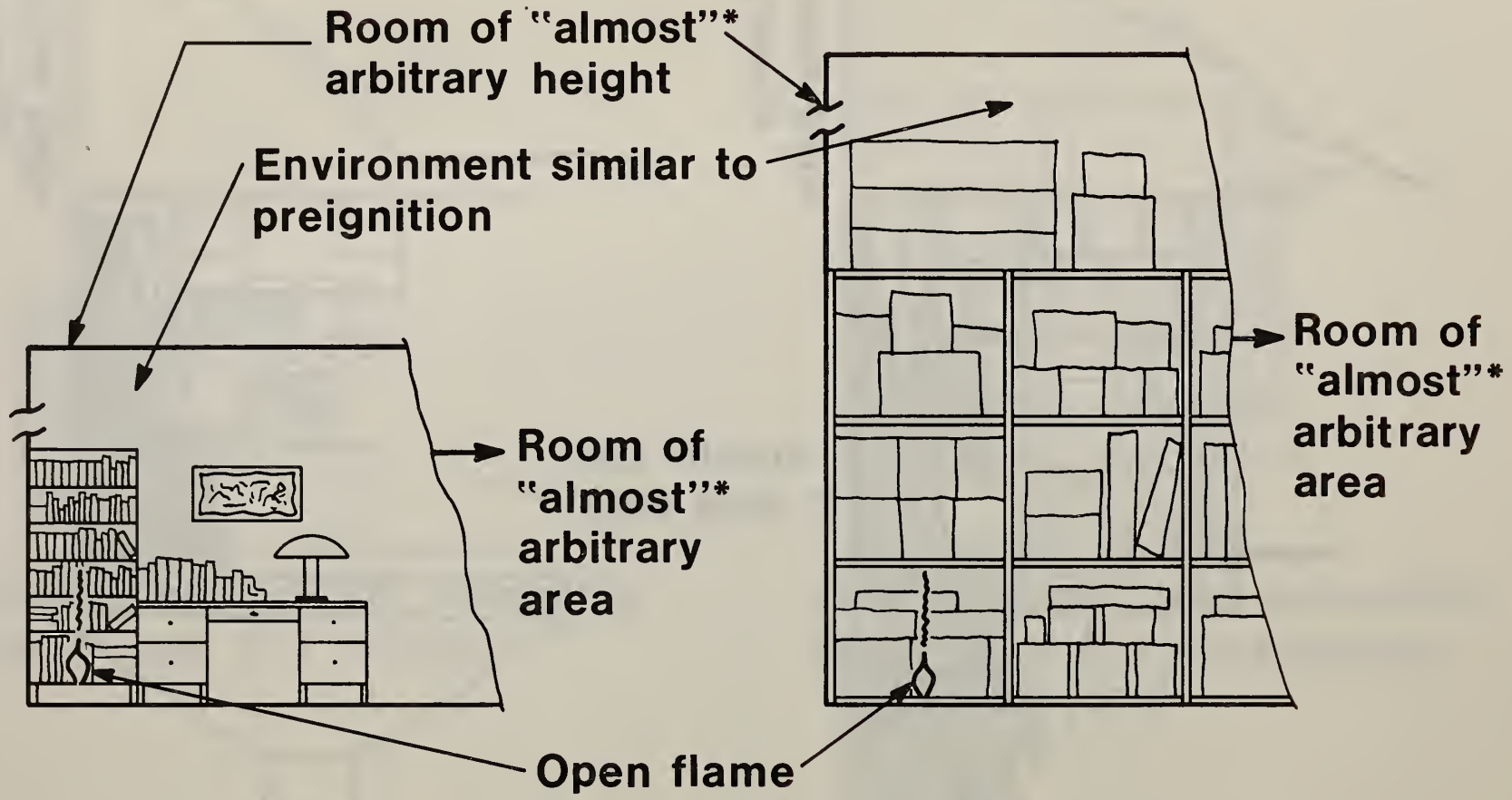

- ~10 kW energy release rate from ignition source
- Energy release rate history will remain close to that of free burn test beyond predicted times of intolerably hazardous conditions

Figure 3. Scenario at the time of ignition

$t = t_{DET}$

- Plume has formed
- Layer has developed and grown in thickness and temperature
- Criterion for detection is satisfied

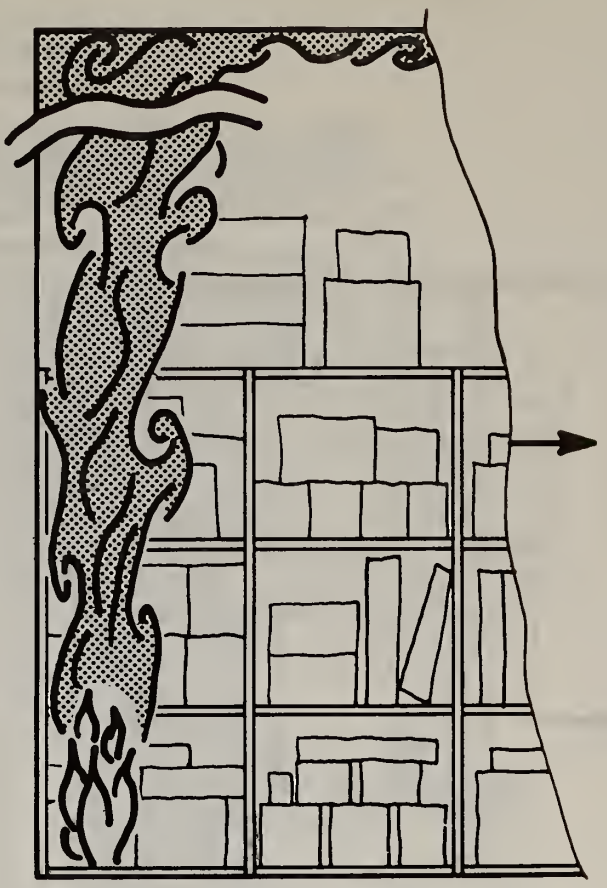

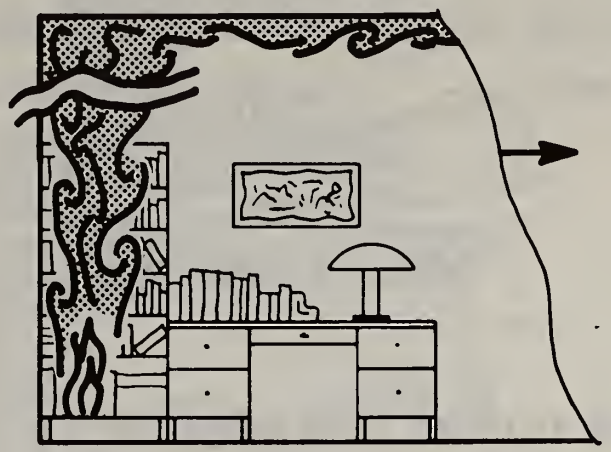

- Possible detection criteria:
  - Thickness of layer
  - Time subsequent to ignition
  - Temperature of layer
  - Rate of temperature rise of layer
  - Other

Figure 4. Scenario at the time of detection

$t = t_{INTERMEDIATE}$

- Layer thickness and temperature continue to grow
- Energy release rate continues to be very close to that of free burn test
- Safe evacuation is still possible

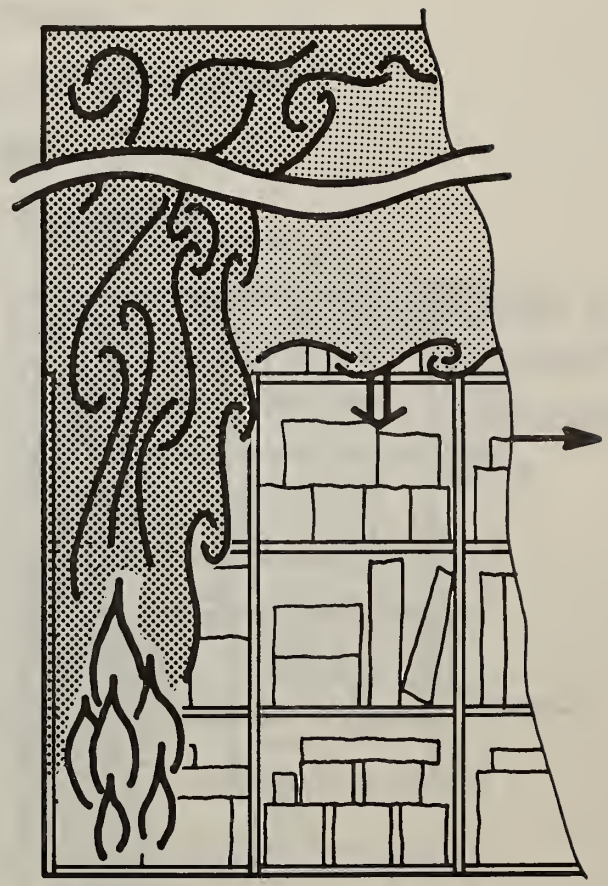

Figure 5. Scenario at intermediate times - between detection and hazard

$t = t_{HAZ}$

- Conditions become hazardous beyond human tolerability
- Hazard criteria:
  - Layer too close to floor for safe condition, or
  - Radiation from layer exceeds safe bounds

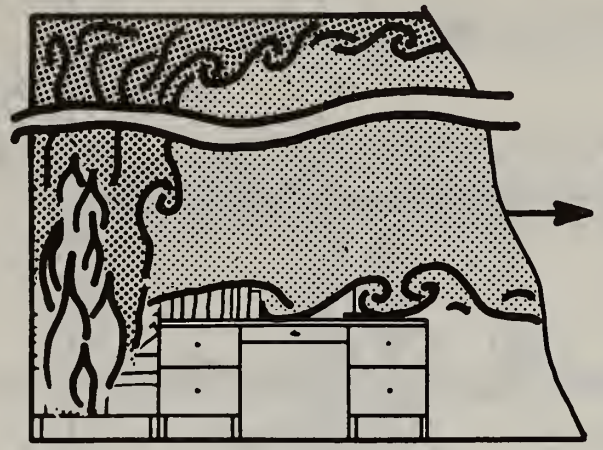

Hot layer drops to critical height - conditions (may be) intolerable for safe evacuation

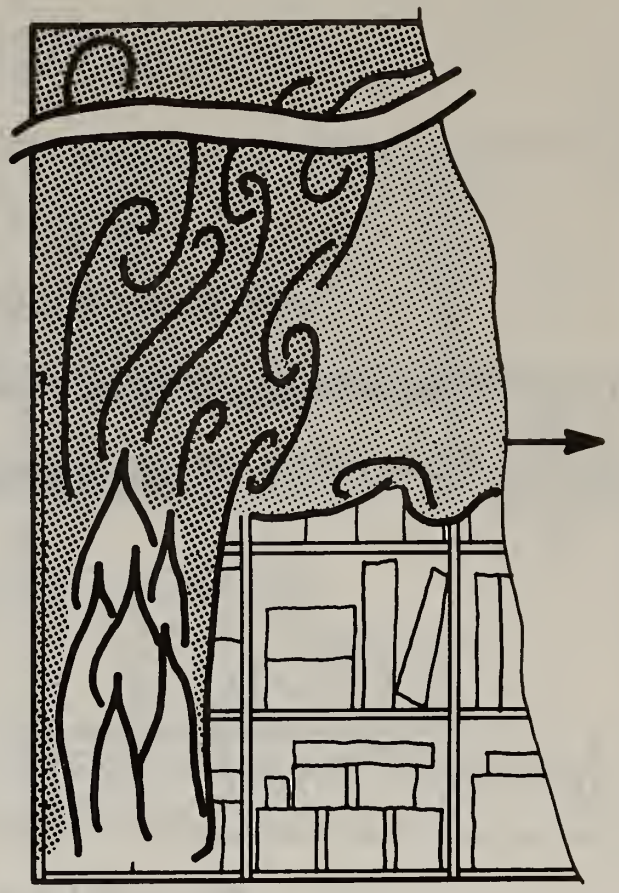

Upper layer temperature becomes critical - radiation exceeds bounds of human tolerability

Figure 6. Scenario at the onset of hazardous conditions

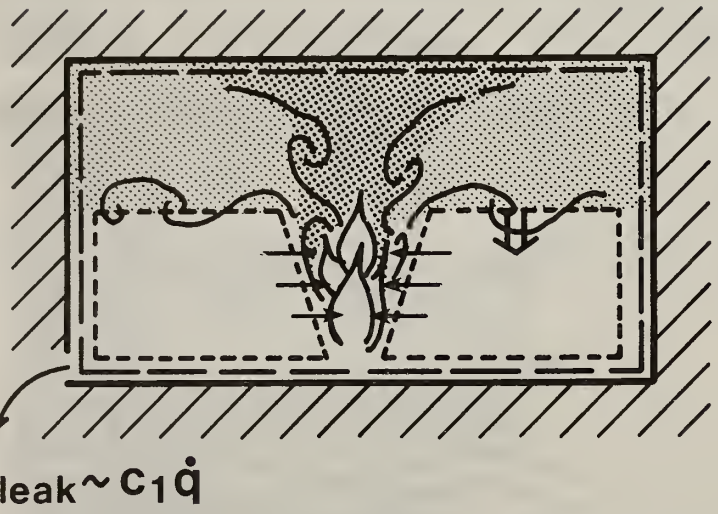

$$\frac{d\zeta}{d\tau} = -c_1\dot{q} - c_2\dot{q}^{1/3}\zeta^{5/3}$$

$$\frac{d\phi}{d\tau} = \frac{\phi\left[c_1\dot{q} - (\phi-1)c_2\dot{q}^{1/3}\zeta^{5/3}\right]}{(\zeta-\zeta_o)}$$

ζ = dimensionless elevation of interface

$\phi = T_{upper}/T_\infty$ = dimensionless layer temperature

q = dimensionless energy release

$c_1 \sim (1-\lambda_c)$; $c_2 \sim (1-\lambda_r)^{1/3}$

Figure 7. Simple illustration of fire-in-enclosure flow dynamics

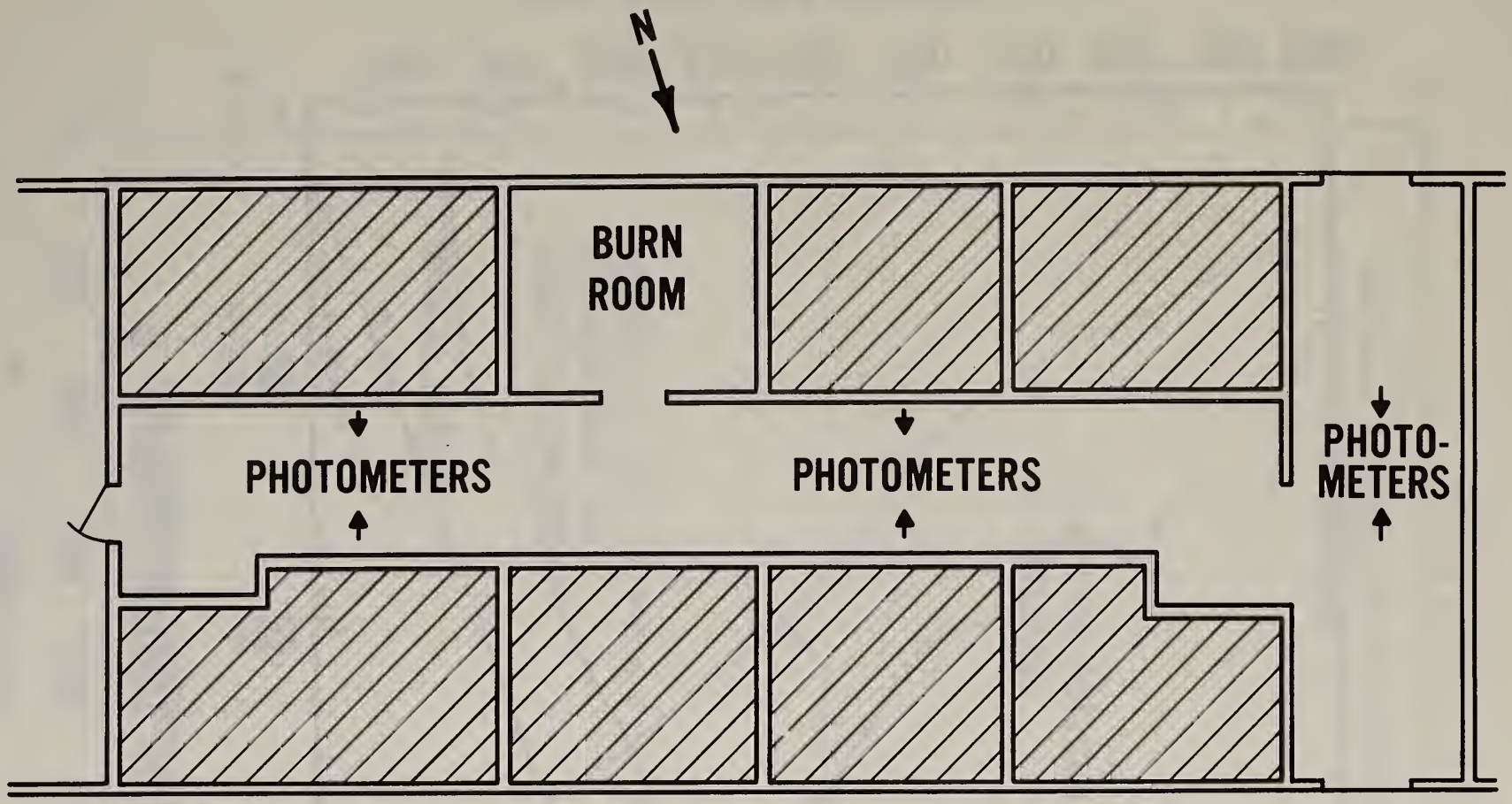

Figure 8. Plan view of hospital room - corridor mockup space

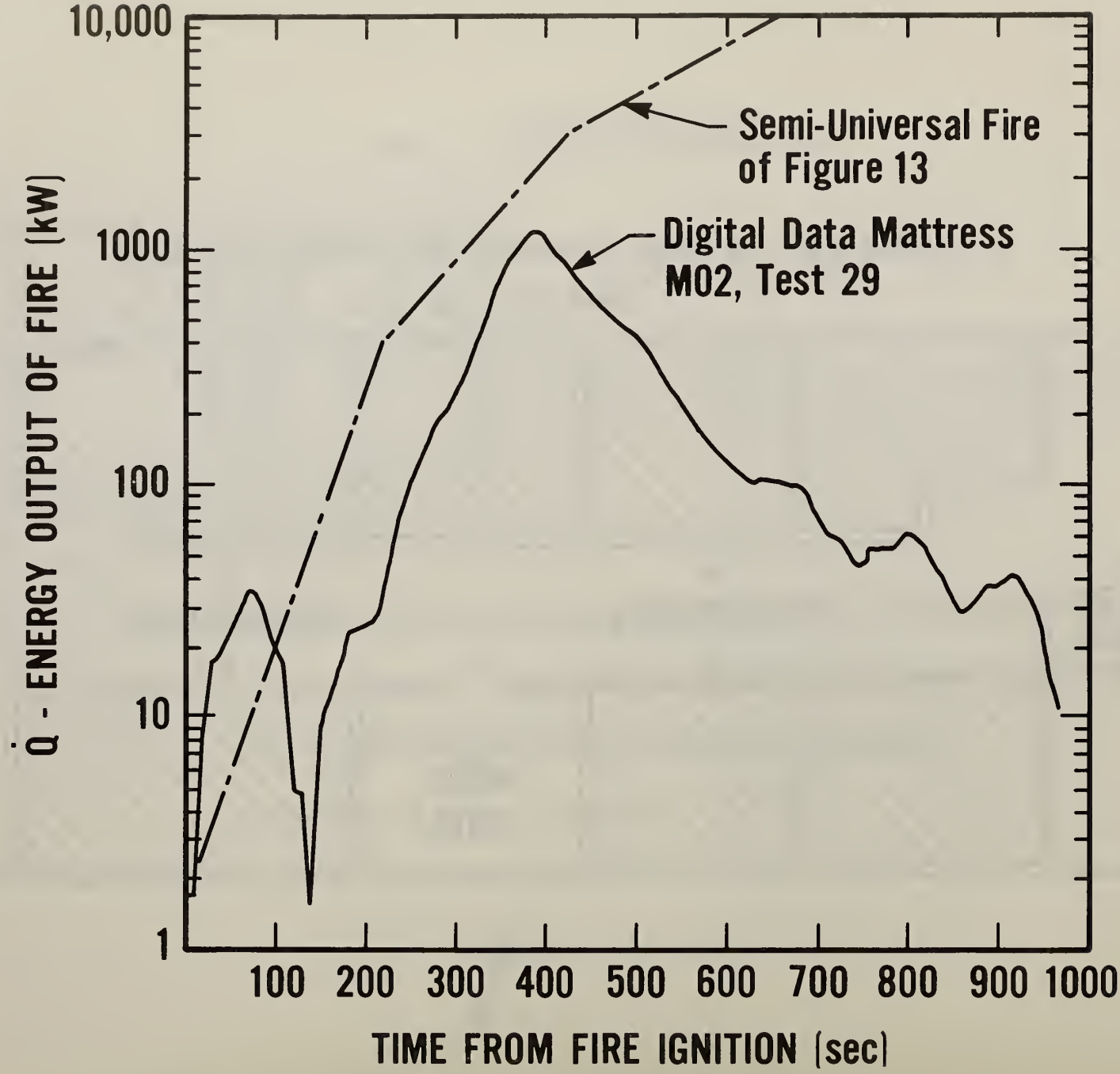

Figure 9. Energy release rate of wastepaper basket - mattress fuel assembly

Figure 10. History of interface position

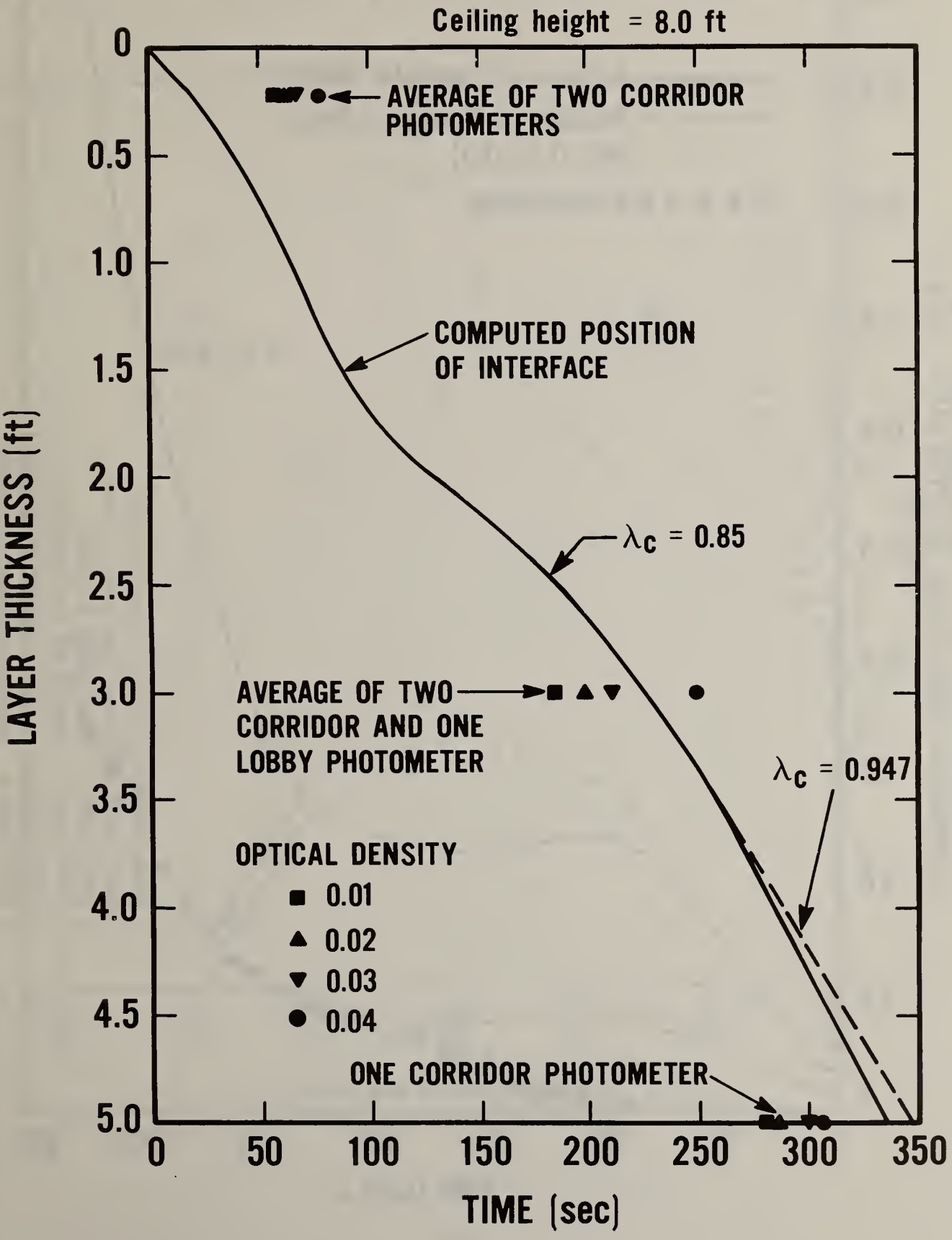

Figure 11. History of average upper layer temperature

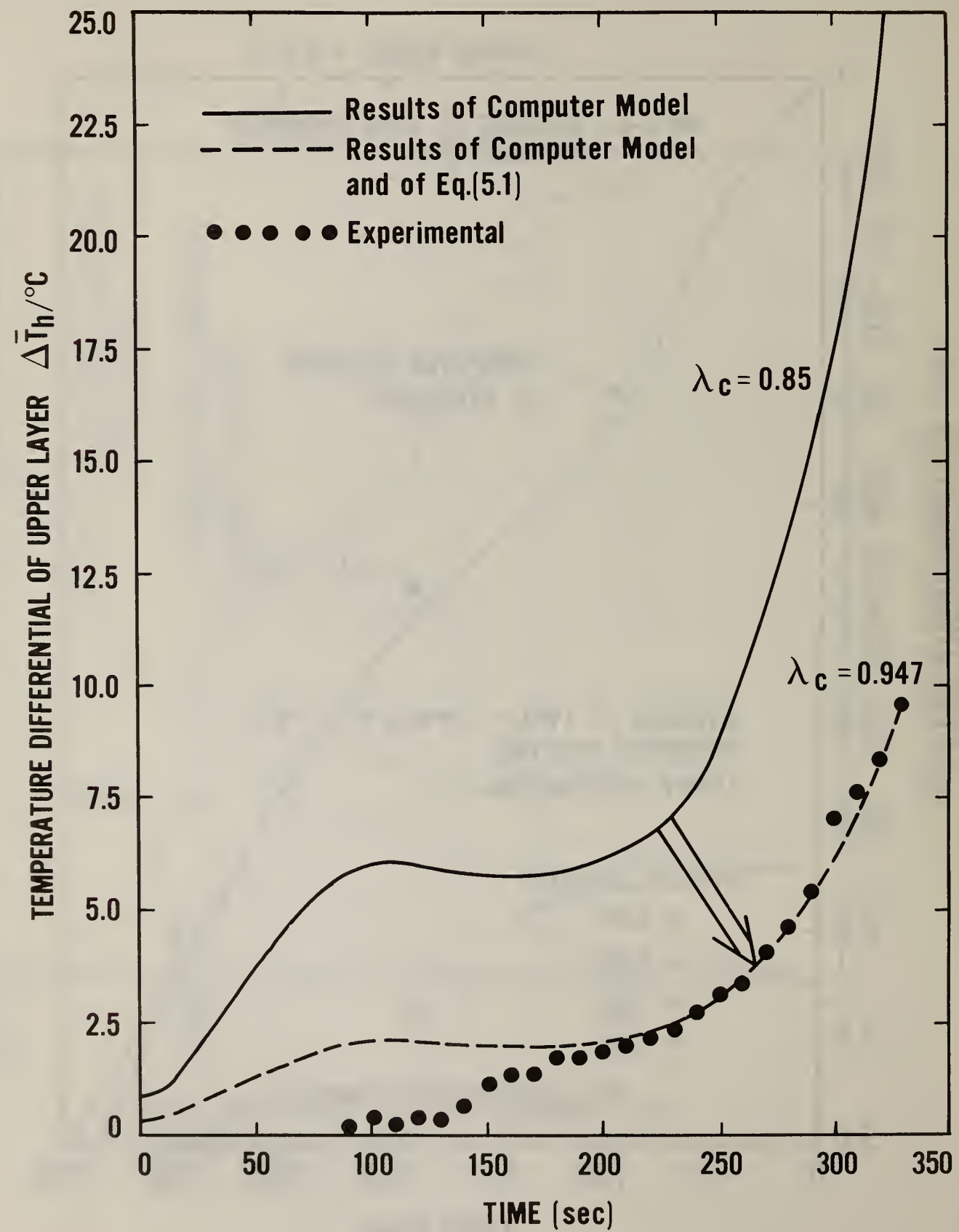

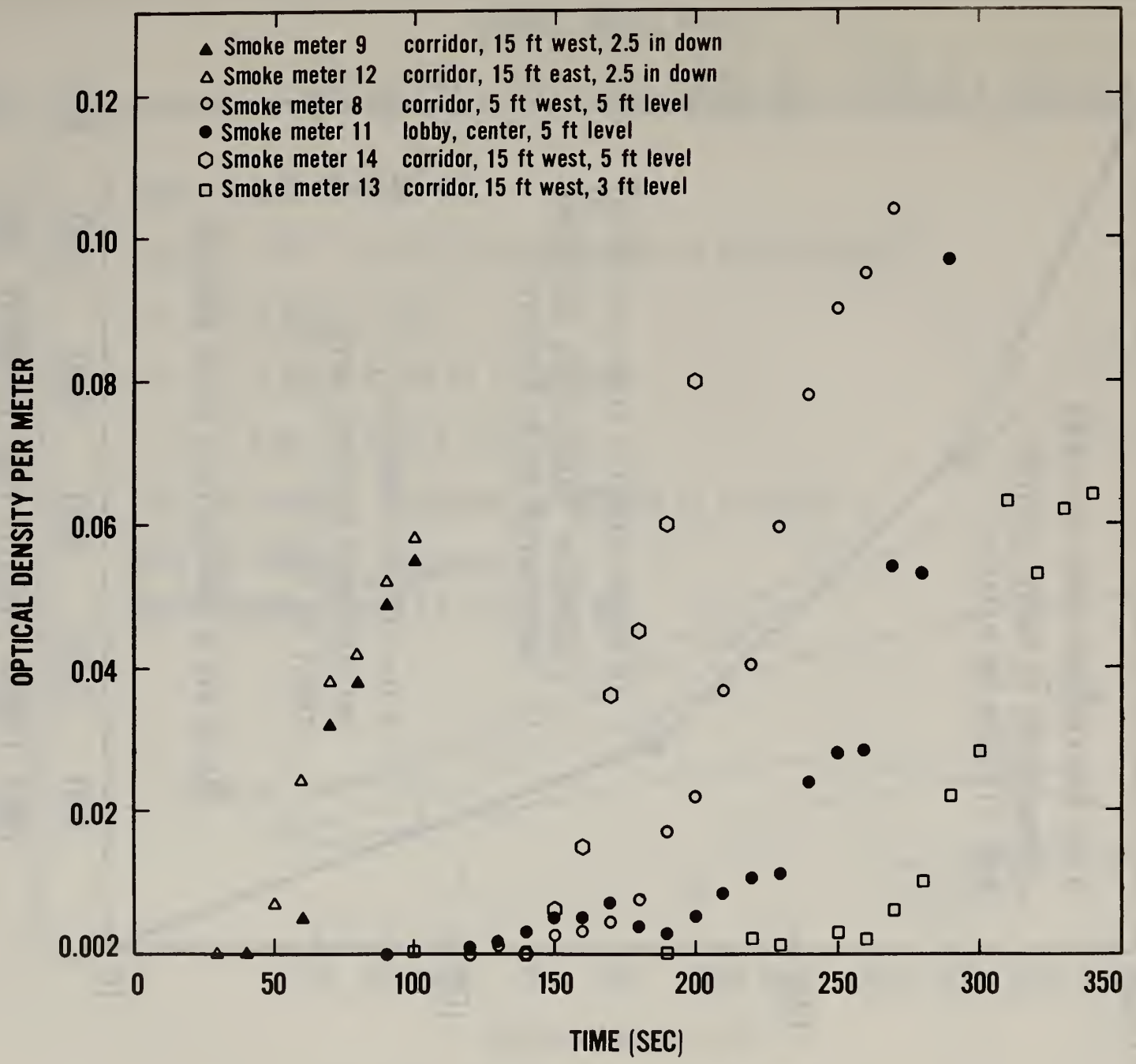

Figure 12. Optical densities measured by the photometers

Figure 13. Free burn energy release rate from a semi-universal fire. A fictitious construct from the data of Friedman [1]

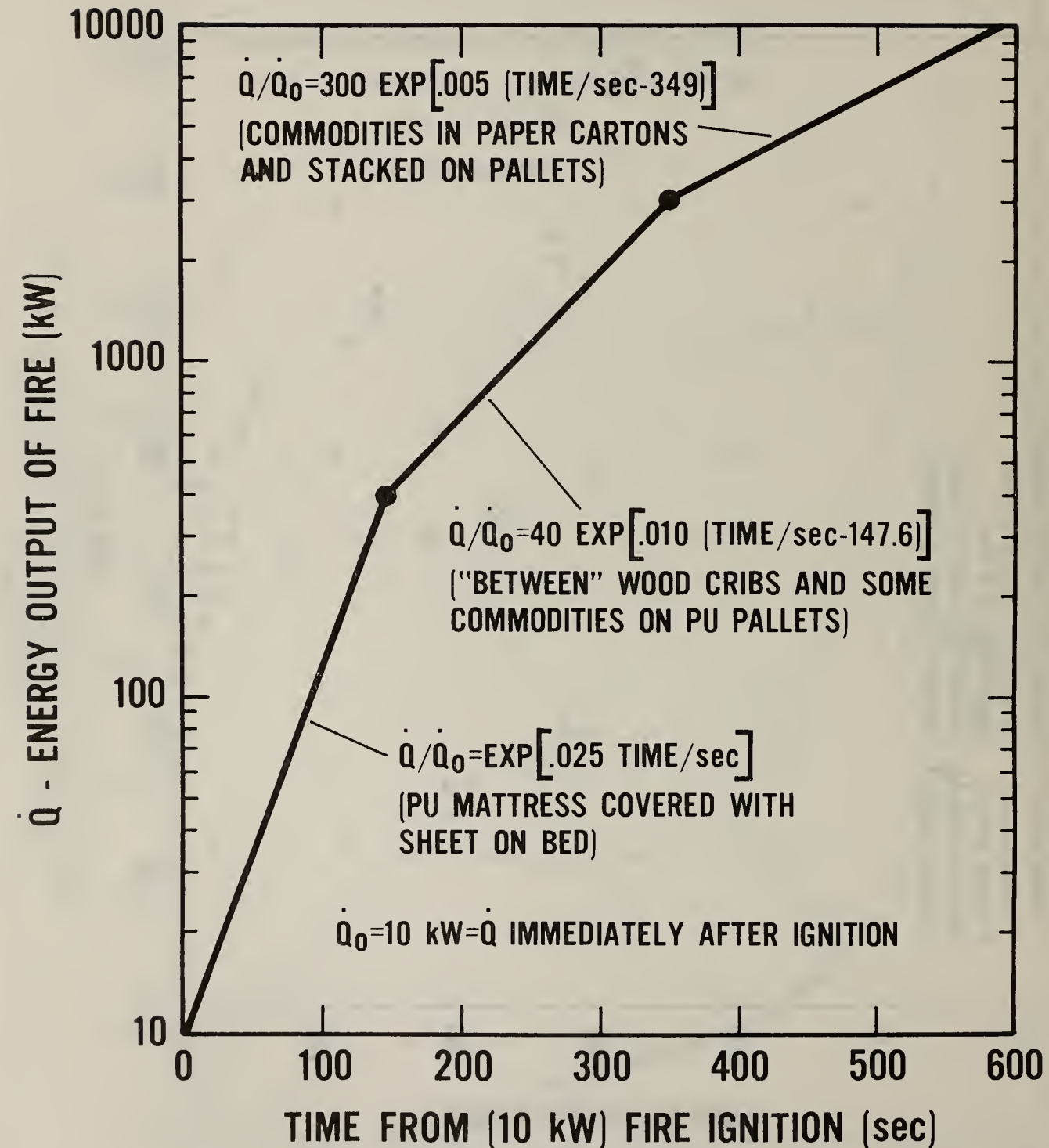

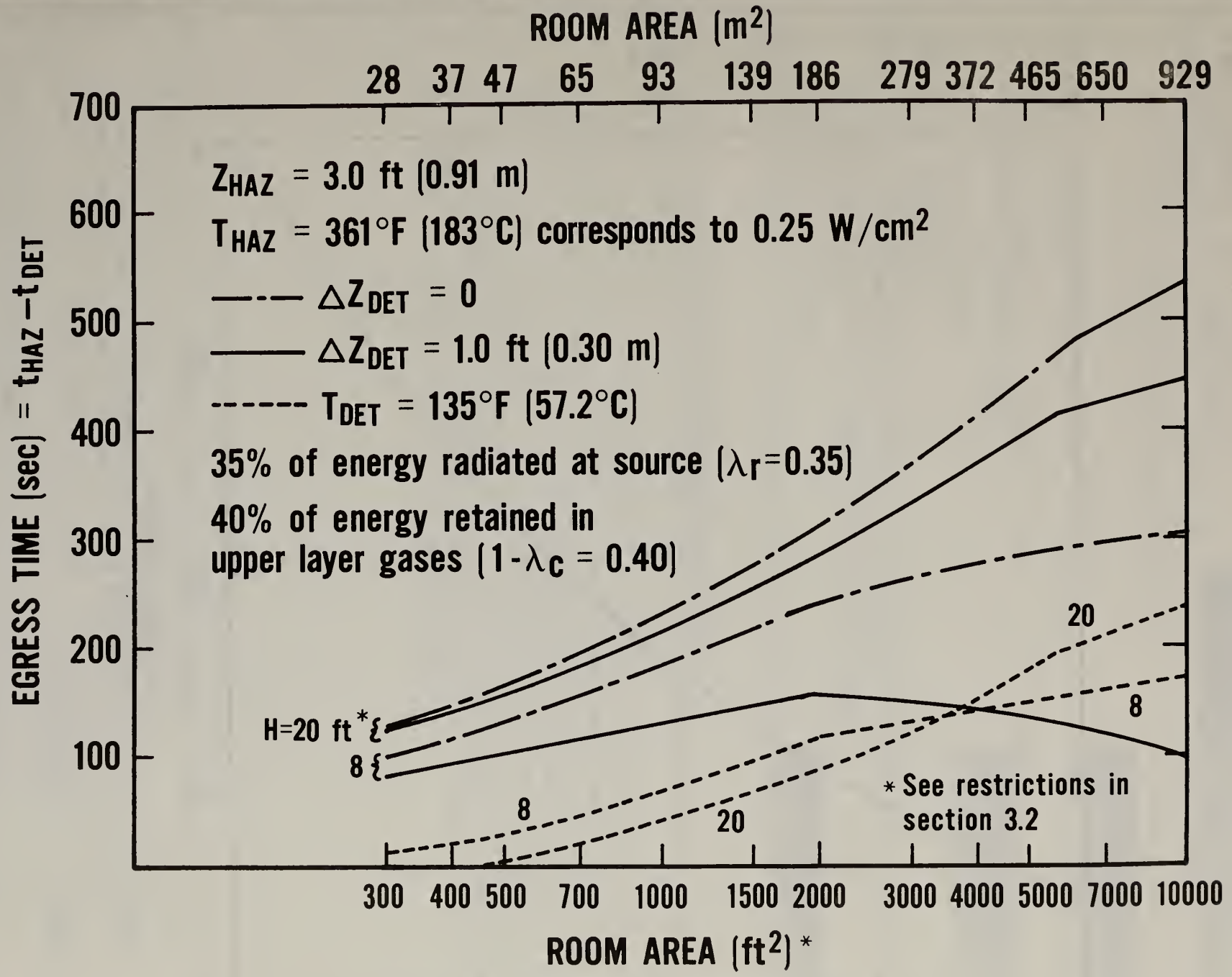

Figure 14. Estimates of available egress times from the semi-universal fire of figure 13

Figure 15. Plot of $\lambda_{ceiling}/(1-\lambda_r)$ as a function of r/H

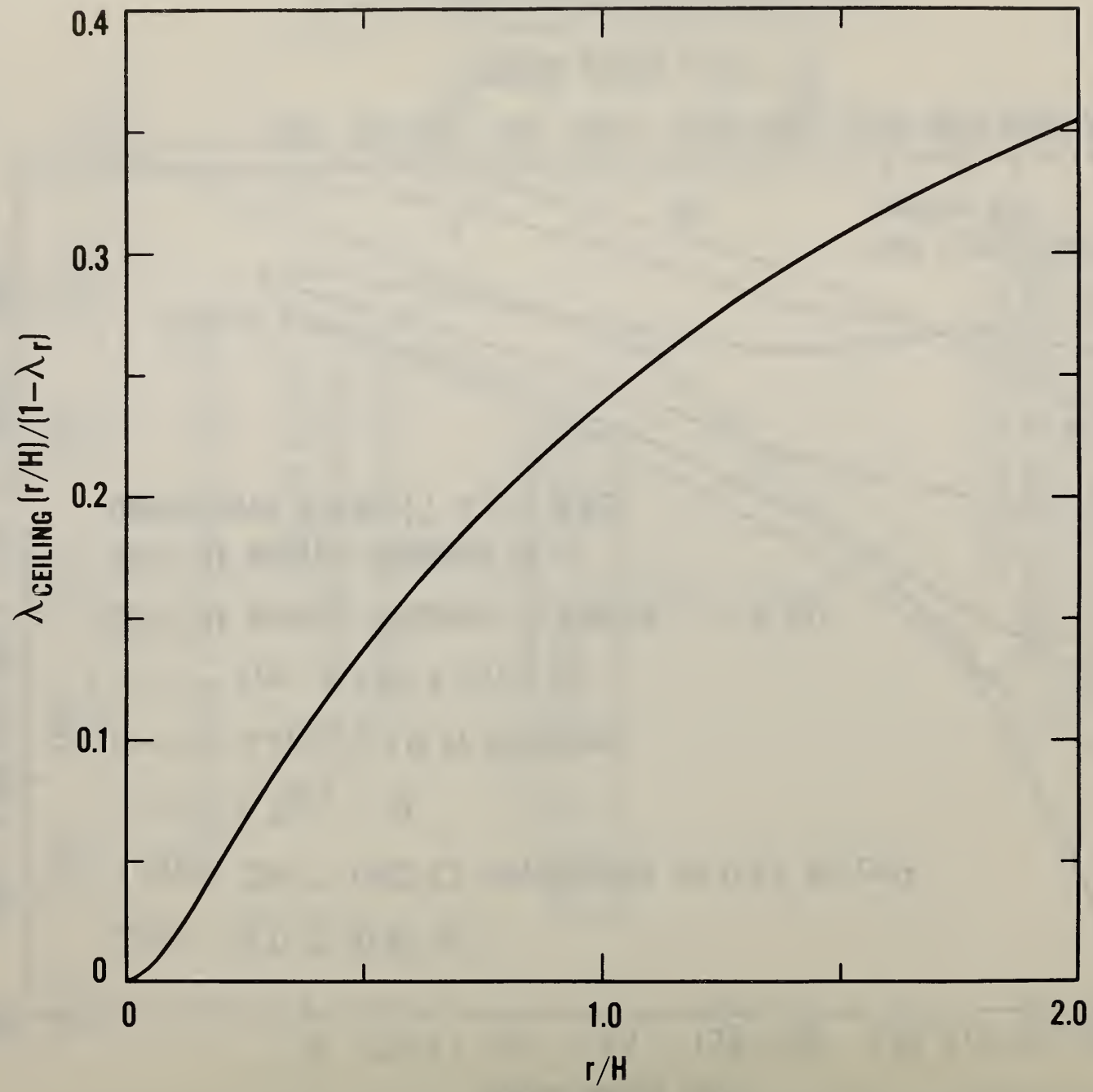

NBS-114A (REV. 9-78)

U.S. DEPT. OF COMM. BIBLIOGRAPHIC DATA SHEET	1. PUBLICATION OR REPORT NO. NBSIR 80-2172	2. Gov't. Accession No.	3. Recipient's Accession No.

4. TITLE AND SUBTITLE

ESTIMATING SAFE AVAILABLE EGRESS TIME FROM FIRES

5. Publication Date

February 1981

6. Performing Organization Code

7. AUTHOR(S)

Leonard Y. Cooper

8. Performing Organ. Report No.

9. PERFORMING ORGANIZATION NAME AND ADDRESS

NATIONAL BUREAU OF STANDARDS
DEPARTMENT OF COMMERCE
WASHINGTON, DC 20234

10. Project/Task/Work Unit No.

11. Contract/Grant No.

12. SPONSORING ORGANIZATION NAME AND COMPLETE ADDRESS *(Street, City, State, ZIP)*

The Occupational Safety and Health Administration (OSHA)
Department of Labor
Washington, D. C. 20210

13. Type of Report & Period Covered

Final

14. Sponsoring Agency Code

15. SUPPLEMENTARY NOTES

☐ Document describes a computer program; SF-185, FIPS Software Summary, is attached.

16. ABSTRACT *(A 200-word or less factual summary of most significant information. If document includes a significant bibliography or literature survey, mention it here.)*

A general technique for estimating the time available for safe egress from a fire is presented. By introducing a qualitative and quantitative model of hazard development, the details of the technique are formulated for the room of fire origin problem. The inputs to the model are the area and ceiling height of the room, data from free burn tests of characteristic fuel assemblies likely to be found therein, the anticipated model of fire detection, and a criterion for the onset of untenability. The output is an estimate of the length of time between detection of a fire and the onset of untenable conditions. Results of applying the estimation technique are presented and discussed.

17. KEY WORDS *(six to twelve entries; alphabetical order; capitalize only the first letter of the first key word unless a proper name; separated by semicolons)*

Combustion products; compartment fires; egress; fire detection; fire growth; hazard analysis; mathematical models; room fires; smoke movement; tenability limits.

18. AVAILABILITY

☒ Unlimited

☐ For Official Distribution. Do Not Release to NTIS

☐ Order From Sup. of Doc., U.S. Government Printing Office, Washington, DC 20402, SD Stock No. SN003-003-

☒ Order From National Technical Information Service (NTIS), Springfield, VA. 22161

19. SECURITY CLASS (THIS REPORT)

UNCLASSIFIED

20. SECURITY CLASS (THIS PAGE)

UNCLASSIFIED

21. NO. OF PRINTED PAGES

72

22. Price

$8.00

USCOMM-DC